

NOTE TO USERS

This reproduction is the best copy available.

UMI[®]



Université d'Ottawa • University of Ottawa



Université d'Ottawa - University of Ottawa

FACULTÉ DES ÉTUDES SUPÉRIEURES
ET POSTDOCTORALES

FACULTY OF GRADUATE AND
POSTDOCTORAL STUDIES

Stéphanie POON

AUTEUR DE LA THÈSE - AUTHOR OF THESIS

M. Sc. (Microbiology and Immunology)

GRADE - DEGREE

Department of Biochemistry, Microbiology and Immunology

FACULTÉ, ÉCOLE, DÉPARTEMENT - FACULTY, SCHOOL, DEPARTMENT

TITRE DE LA THÈSE - TITLE OF THE THESIS

Novel Lamin A/C Mutations and their Expression in the Cardiac Tissue of End-stage Dilated Cardiomyopathy Patients

F. Tesson

DIRECTEUR DE LA THÈSE - THESIS SUPERVISOR

CO-DIRECTEUR DE LA THÈSE - THESIS CO-SUPERVISOR

EXAMINATEURS DE LA THÈSE - THESIS EXAMINERS

H. McBride

B. Tuana

J.-M. De Koninck, Ph.D.

LE DOYEN DE LA FACULTÉ DES ÉTUDES
SUPÉRIEURES ET POSTDOCTORALES

DEAN OF THE FACULTY OF GRADUATE
AND POSTDOCTORAL STUDIES

**NOVEL LAMIN A/C MUTATIONS AND THEIR EXPRESSION
IN THE CARDIAC TISSUE OF
END-STAGE DILATED CARDIOMYOPATHY PATIENTS**

By

STEPHANIE POON, Hon. B.Sc.

A Thesis

Submitted to the School of Graduate Studies

For the Degree

Master of Science

University of Ottawa

© Copyright by Stephanie Poon, September 2003



Library and
Archives Canada

Bibliothèque et
Archives Canada

Published Heritage
Branch

Direction du
Patrimoine de l'édition

395 Wellington Street
Ottawa ON K1A 0N4
Canada

395, rue Wellington
Ottawa ON K1A 0N4
Canada

Your file *Votre référence*
ISBN: 0-494-01581-0
Our file *Notre référence*
ISBN: 0-494-01581-0

NOTICE:

The author has granted a non-exclusive license allowing Library and Archives Canada to reproduce, publish, archive, preserve, conserve, communicate to the public by telecommunication or on the Internet, loan, distribute and sell theses worldwide, for commercial or non-commercial purposes, in microform, paper, electronic and/or any other formats.

The author retains copyright ownership and moral rights in this thesis. Neither the thesis nor substantial extracts from it may be printed or otherwise reproduced without the author's permission.

AVIS:

L'auteur a accordé une licence non exclusive permettant à la Bibliothèque et Archives Canada de reproduire, publier, archiver, sauvegarder, conserver, transmettre au public par télécommunication ou par l'Internet, prêter, distribuer et vendre des thèses partout dans le monde, à des fins commerciales ou autres, sur support microforme, papier, électronique et/ou autres formats.

L'auteur conserve la propriété du droit d'auteur et des droits moraux qui protègent cette thèse. Ni la thèse ni des extraits substantiels de celle-ci ne doivent être imprimés ou autrement reproduits sans son autorisation.

In compliance with the Canadian Privacy Act some supporting forms may have been removed from this thesis.

Conformément à la loi canadienne sur la protection de la vie privée, quelques formulaires secondaires ont été enlevés de cette thèse.

While these forms may be included in the document page count, their removal does not represent any loss of content from the thesis.

Bien que ces formulaires aient inclus dans la pagination, il n'y aura aucun contenu manquant.


Canada

ABSTRACT

Dilated cardiomyopathy (DCM) is a cardiac muscle disorder characterized by ventricular dilatation and impaired systolic function. LMNA, one of fifteen autosomal genes implicated in this disease, encodes for two alternatively spliced nuclear intermediate filaments proteins, lamins A and C.

Two novel missense mutations, D192G and R541S, were identified in highly conserved regions of the LMNA gene. Electron micrographs of cardiac tissue containing the D192G mutation demonstrated dramatic morphologic alterations of the nucleus. By contrast, cardiac samples from the R541S carrier were almost indistinguishable from those of transplanted DCM patients without LMNA mutations. Expression levels of total LMNA mRNA in this individual were comparable to those found in end-stage DCM patients without LMNA mutations. Moreover, the mutated allele was expressed in the heart tissue of this patient. Functional studies to determine the impact of these mutations on cellular models are ongoing.

ACKNOWLEDGEMENTS

Although I am now in my second year of medicine at Queen's University, I must admit that completing this thesis has been one of the most memorable and challenging experiences of my life. I would like to extend my appreciation and gratitude to those who have seen me through to the end of this incredible journey.

First of all, I would like to express thanks to Dr. Mezl, who showed me that there is always a way if there is a will. Without his support, I would never have gained the opportunity to complete my research and continue my studies in medicine simultaneously. I am especially grateful to Carol Ann Kelly for her indispensable advice and ever-ready willingness to lend a helping hand.

The members of my advisory committee, Dr. Dennis Bulman and Dr. Nancy Carson, are also to be commended for finding the time to facilitate and guide me through this entire process in the midst of their very busy schedules.

I would also like to express a heartfelt thanks to the members of the genetics lab at the University of Ottawa Heart Institute. Their friendship and support made this a truly positive and enriching experience. I am especially indebted to Pierrette Bolongo for her patience and wisdom. She was an invaluable mentor who taught me not only the fundamentals of genetic procedures, but also the value of perseverance. In addition, I would like to thank André Gauthier for his insightful instruction on the LightCycler and for generously sharing his resources and experience.

It has been a great pleasure to work for and with Dr. Frédérique Tesson. She has been the light in the dark tunnel of my ignorance, and I hold her in the greatest esteem as a scientist and supervisor.

I would also like to acknowledge the contributions made by our collaborators:
Drs. Bilinska and Ruzylo from the National Institute of Cardiology in Warsaw, Poland;
Dr. Veinot, from the University of Ottawa; and Dr. Fidzianska, from the Polish Academy
of Science in Warsaw, Poland.

Last, but definitely not least, I would like to dedicate this thesis to my parents and
friends. Without their unconditional love, support, and understanding, I would never
have been able to come so far and achieve so much. They were my motivation and my
inspiration during the times when I sorely lacked both, and when I do manage to cross
this finish line some day in the future, I will owe it all to their unwavering dedication and
encouragement.

TABLE OF CONTENTS

1	INTRODUCTION	1
1.1	Dilated Cardiomyopathy	1
1.2	Clinical and Genetic Heterogeneity of Dilated Cardiomyopathy	3
1.3	Familial DCM Genes	3
1.3.1.	Sarcomeric Proteins	4
1.3.2.	Cytoskeletal Proteins	8
1.3.3.	Other Proteins Implicated in DCM	10
1.4	Lamin Function	13
1.4.1.	Nuclear Organization	13
1.4.2.	Anchorage Sites for Chromatin	14
1.4.3.	DNA Replication	15
1.4.4.	RNA Polymerase II Transcription	16
1.4.5.	Signal Transduction	17
1.5	Lamin Mutations and Disease	17
1.5.1.	Emery-Dreifuss Muscular Dystrophy (EDMD)	17
1.5.2.	Limb Girdle Muscular Dystrophy (LGMD)	19
1.5.3.	Dunnigan-Type Familial Partial Lipodystrophy	20
1.5.4.	Charcot-Marie-Tooth Disorder Type 2 (CMT2)	22
1.5.5.	Mandibuloacral Dysplasia (MAD)	22
1.5.6.	Hutchison-Gilford Progeria Syndrome	23
1.5.7.	Dilated Cardiomyopathy	24
1.6	Statement of Objectives	25

2	MATERIALS AND METHODS.....	26
2.1	Patient Population	26
2.2	Tissue Collection	27
2.3	DNA Extraction	28
2.4	Genomic DNA Amplification.....	28
2.5	Single Strand Conformation Polymorphism (SSCP).....	29
2.6	Denaturing High Performance Liquid Chromatography (DHPLC).....	29
2.7	DNA Sequencing	30
2.8	Electron Microscopy.....	30
2.9	RNA Extraction	30
2.10	Quantitative RT-PCR.....	31
2.11	Restriction Fragment Length Polymorphism (RFLP) Analysis.....	32
3	RESULTS	33
3.1	Identification of Novel LMNA Mutations in DCM Patients.....	33
3.1.1	Patient 1	33
3.1.1.1	Family History.....	33
3.1.1.2	Mutation Analysis.....	35
3.1.2	Patient 2	39
3.1.2.1	Family History	39
3.1.2.2	Mutation Analysis.....	39
3.2	Determination of the Expression of the Novel LMNA Mutations in Cardiac Tissue from DCM Patients	42
3.2.1	Electron Microscopy.....	42

3.2.2	Comparison of LMNA Expression in the Left Ventricle of End-Stage DCM Patients With or Without LMNA Mutations	45
3.2.3	Determination of the Relative Expression of the Wild-type vs the Mutated LMNA Allele in the Cardiac Tissue from Patient 2 and a LMNA Wild-type, End-Stage DCM Patient.....	49
4	DISCUSSION.....	52
4.1	LMNA Mutations and Dilated Cardiomyopathy	52
4.2	The Identification of Novel LMNA Mutations in DCM	56
4.2.1	Lamin A/C Gene and Protein.....	56
4.2.2	Location of Lamin A/C Mutations.....	57
4.3	Effect of LMNA Mutations on the Nuclear Architecture of Cardiac Myocytes from End-Stage DCM Patients.....	59
4.4	Expression of the Wild-Type vs. the Mutated Allele in the Cardiac Tissue of End-Stage DCM Patients With or Without LMNA Mutations	62
4.5	Model Mechanisms for Autosomal Dominance of LMNA Mutations.....	63
4.6	Pathogenic Mechanisms of LMNA Mutations	67
4.6.1	Mechanical Stress Model.....	67
4.6.2	Gene Expression Model.....	68
4.6.3	Putative Models of Pathogenesis for the D192G and R541S Mutations Expressed in End-Stage DCM Patients	70
4.7	Phenotypic Diversity of LMNA Mutations and the Role of Modifier Genes	72
4.8	Study Limitations.....	75

4.9	Clinical Implications.....	77
4.10	Future Directions	78
5	CONCLUSION.....	81
	REFERENCES	82
6	CONTRIBUTIONS OF COLLABORATORS.....	92
	APPENDICES	93
	CURRICULUM VITAE.....	98

LIST OF ABBREVIATIONS

A	Alanine
ACN	Acetonitrile
BAF	Barrier to autointegration factor
bp	Base pairs
C	Cysteine
Ca ²⁺	Calcium
CMT2	Charcot-Marie-Tooth Disorder type 2
Col I	Collagen I
Col III	Collagen III
CPK	Creatine phosphokinase
D	Aspartic acid
DCM	Dilated cardiomyopathy
DHPLC	Denaturing high performance liquid chromatography
E	Glutamic acid
EDMD	Emery-Dreifuss muscular dystrophy
EDTA	Ethylene diamine tetraacetic acid
ER	Endoplasmic reticulum
FPLD	Familial partial lipodystrophy
FS	Frameshift

G	Glycine
G4.5	Tafazzin
GAPDH	glyceraldehyde-3-phosphate dehydrogenase
H	Histidine
HDL	High-density lipoprotein
HGPS	Hutchison-Gilford progeria syndrome
INM	Inner nuclear membrane
K	Lysine
L	Leucine
LAP	Lamina-associated peptide
LGMD	Limb girdle muscular dystrophy
LMNA	Lamin A/C gene
M	Molar
MAD	Mandibuloacral dysplasia
MEF	Mouse embryonic fibroblast
μg	Microgram
MgCl ₂	Magnesium chloride
μl	Microliter
mL	Milliliter
MLP	Cysteine-and glycine-rich protein 3
μM	Micromolar
mM	Millimolar
MYBPC	Cardiac myosin-binding protein C

N	Asparagine
ng	Nanogram
nm	Nanometer
NPC	Nuclear pore complex
ONM	Outer nuclear membrane
P	Proline
p110Rb	Retinoblastoma protein
PAF	Platelet-activating factor
PCR	Polymerase chain reaction
pg	Picograms
PKA	Protein kinase A
PKC	Protein kinase C
PLN	Phospholamban
R	Arginine
RFLP	Restriction fragment length polymorphism
RT-PCR	Reverse transcriptase polymerase chain reaction
S	Serine
SERCA2	Sarcoplasmic reticular calcium-adenosine triphosphatase pump
SGCD	Delta-sarcoglycan gene
SREBP1	Sterol-response element-binding protein 1
SSCP	Single strand conformation polymorphism
STA	Emerin gene
TEAA	Triethylammonium acetate

t_r	Retention time
U	Units
vs.	Versus
W	Tryptophan
WT	Wild-type
X	Stop codon
Y	Tyrosine
YA	Young Arrest

LIST OF FIGURES AND ILLUSTRATIONS

- Fig. 1 Partial Pedigree of Patient 1
- Fig. 2 DHPLC Analysis of LMNA exon 3 in Patient 1 and Control Samples
- Fig. 3 DNA Sequencing Electropherograms of LMNA exon 3 from Patient 1 and Control DNA
- Fig. 4 Location of the D192G Mutation Within the Secondary Structure of Human LMNA.
- Fig. 5 Partial Pedigree for Patient 2
- Fig. 6 SSCP Analysis of LMNA exon 10 from Patient 2 and a Control DNA Sample at 10°C and 20°C
- Fig. 7 DNA Sequencing Electropherograms of LMNA exon 10 from Patient 2 and Control DNA
- Fig. 8 Location of the R541S Mutation Within the Secondary Structure of Human LMNA
- Fig. 9 Electron Micrographs of the Nuclear Membrane in LMNA Mutant and Wild-Type Cardiomyocytes
- Fig. 10 Standard Dilution Curves for LightCycler Analysis of GAPDH and LMNA exon 10
- Fig. 11 SYBR Green RT-PCR Quantification of LMNA mRNA in the Heart Tissue Samples from Patient 2 and Two Wild-Type LMNA End-Stage DCM Patients
- Fig. 12 Cleavage of R541S and Wild-type LMNA cDNA by HinP1

Fig. 13 R541S Allele Expression in Heart Tissue from Patient 2 Determined by
HinP1 RFLP

Fig. 14 Localization of Published LMNA Mutations in DCM

1 INTRODUCTION

1.1 Dilated Cardiomyopathy

The term “cardiomyopathy” represents a diverse group of heart-muscle disorders. In response to cardiovascular disease, the morphology of the heart is remodeled as a compensatory mechanism to preserve pump function (1). More than 80% of cardiomyopathies are classified as dilated or congestive (2). Population surveys estimate that approximately 36.5 in 100,000 people are affected by dilated cardiomyopathy (DCM) (3). DCM is characterized by the progressive dilation of the left, or both, ventricles and impaired systolic function (4). Ventricular dilation is almost always accompanied by modest increases in ventricular wall thickness, which reflects myocyte hypertrophy as well as variable increases in interstitial fibrosis. However, the maximal left ventricular free-wall thickness and septal thickness are typically normal because of the abnormally dilated chambers (5). Pathologic manifestations are often nonspecific (1). Although microscopic examination of the myocardium may reveal no evidence of abnormal histopathology (1), the ratio of collagen I (Col I) to collagen III (Col III) appears to be increased in DCM patients (6). This may account for the augmented amount of fibrosis and may contribute to the systolic dysfunction in DCM (6). Diminished contractile function is the critical hemodynamic feature of DCM, an abnormality that triggers complex neurohumoral responses, which increase circulatory volume so as to maintain cardiac output (2).

While compensatory mechanisms are initially beneficial to heart function, they may ultimately become maladaptive. Hypertrophic and dilated cardiac morphologies

increase myocardial strain, raise metabolic demands and, by impeding ventricular relaxation, may compromise coronary artery blood flow (1). Cardiac remodeling can therefore accelerate functional deterioration and the onset of heart failure, serious arrhythmias and thromboembolic events, all of which account for the substantial morbidity and premature mortality of this disease (1). Indeed, only 50% of patients with DCM survive more than 5 years after their diagnosis (2). This disease is a significant health problem, as it is often associated with high rates of sudden death and accounts for greater than 50% of all heart transplantation indications (7).

There has been significant progress in delineating the causes of primary cardiomyopathies. Ischemic, alcoholic/toxic, metabolic, or infectious causes of DCM have all been recognized (8-10). However, in many instances, an underlying pathology is not discovered, and the diagnosis of “idiopathic” DCM ensues (2). Over the past two decades, there has been an increased recognition that many of these idiopathic DCM cases are actually familial. Michels and colleagues reported in 1992 that over 20% of individuals with DCM had an affected first-degree relative (3). Since then, the estimated incidence of familial DCM has ranged from 20% to as high as 35-48% (9;11;12). However, the true frequency is probably still underestimated due to the absence of early disease markers and reduced penetrance (10). Several large population-based studies have confirmed these data and have delineated that DCM can be transmitted as autosomal dominant, autosomal recessive, X-linked, or mitochondrial traits (see Appendix I) (2). However, the mode of inheritance is autosomal dominant in the vast majority (>70%) of DCM families (11).

1.2 Clinical and Genetic Heterogeneity of Dilated Cardiomyopathy

Studies demonstrate that there is a vast clinical and genetic heterogeneity among DCM cases (10). Attempts have been made in the past to place the multiple phenotypes of DCM into various categories (10). However, as the body of knowledge surrounding this disease accumulates over time, it becomes more apparent that the complexity of DCM cannot be reduced into simple generalizations. Age at disease onset ranges from early childhood to late in senescence, although most cases of genetic or acquired DCM become apparent during the fourth or fifth decade of life (2). The severity of symptoms and survival can also vary considerably, even in affected members of the same family with the same mutation (2). In addition, some cases may present with auxiliary cardiac phenotypes and extracardiac findings. This clinical heterogeneity is mirrored by the genetic diversity of DCM. Since 1993, mutations in genes encoding cytoskeletal, contractile, nuclear membrane, and other proteins have been identified in patients with familial and sporadic DCM (13) (see Appendix I). Despite this seemingly expansive inventory of candidate genes, the identities of the disease genes associated with many DCM loci still remain obscure.

1.3 Familial DCM Genes

The candidate genes that have been implicated thus far in the pathogenesis of this disease can be roughly divided into three broad groups, based on the location of the encoded protein within the cardiac myocyte. The first group includes components of the sarcomere, which is the fundamental unit of contraction in all muscle cells. Cytoskeletal proteins comprise the second group, whereas the last category consists of genes that

encode for a variety of other proteins, which are considered to be distinct entities from the constituents of the cardiac cytoarchitecture.

1.3.1 Sarcomeric Proteins

This category of genes includes actin, myosin, cardiac troponin T, alpha-tropomyosin, titin, titin-cap, cysteine-and glycine-rich protein 3 (MLP), and cardiac myosin-binding protein C (MYBPC).

The first gene to be identified for pure DCM was cardiac alpha-actin in 1998 (14). Two mutations were discovered by Olson et al. in the immobilized end of the actin filament (14). Both of these substitutions altered amino acids involved in actin-cytoskeletal, rather than actin-myosin, interactions. The consequences of these mutations were thus believed to consist of a diminution of force transmission from the sarcomere to the cytoskeleton, rather than a deficit in force generation (2;5;15). These novel findings initiated a screening frenzy in various laboratories, but to no avail. Despite multiple attempts to demonstrate otherwise, the cardiac actin gene seemed to be rarely implicated (7;16). Indeed, no mutations were found in subsequent studies of 44 American probands (17), 136 Japanese DCM patients (18), or 57 individuals with DCM of mostly black African origin (19).

However, the discovery that cardiac actin mutations could be linked to the pathology of DCM prompted researchers to search for answers among other sarcomeric proteins, which had previously been implicated in hypertrophic cardiomyopathy. Kamisago et al. discovered two substitutions in myosin that caused early-onset ventricular dilation, diminished contractile function, and heart failure (8). One of the mutations disrupted a highly conserved structure that contributes to the tight binding of

actin, an interaction that is critical for initiating the power stroke of contraction (8). Another mutation was located in the center of the “converter region”, one of several flexible joints in myosin that undergo conformational changes during the contractile cycle (8). This region transmits movement and directionality from the head of myosin to the neck, which assists in propelling the thick filament (8). Substitution of an amino acid at this position may alter the magnitude or polarity of the transmitted movement, and consequently diminish the efficiency of contraction (8). Recently, Daehmlow et al. expanded the list of DCM mutations in this gene by identifying two more substitutions, one of which is expected to alter the binding of myosin to actin (20). Once again, this would lead to a deficit in force production by the sarcomere. Daehmlow et al. also discovered the presence of a missense mutation in the cardiac myosin-binding protein C (MYBPC3) gene, but the functional consequences of this substitution have not been ascertained to date (20).

As a supplement to his earlier work, Kamisago et al. also identified a deletion in the cardiac troponin T gene, which produced the same DCM phenotype as the beta-myosin heavy chain mutations (8). This exact mutation was rediscovered by Hanson et al. two years later in a different study population (21). Essentially, the affected residue is located in a domain containing three conserved lysines (K208-210) that form a tight binary complex with troponin C (8). Loss of K210 would reduce these ionic interactions and diminish the activation of Ca^{2+} -stimulated actomyosin ATPase (8). This would subsequently decrease the power stroke of contraction (8). In 2001, Li et al. reported another mutation within the tropomyosin-binding domain of cardiac troponin T, which was also postulated to impair cardiac contractility (22). This hypothesis was supported

by an experiment in which progressive truncation of the troponin tail correlated with an increasing to virtually complete elimination of troponin-tropomyosin binding to actin (23).

To further test the hypothesis that dysfunction of the sarcomere could lead to either familial hypertrophic or dilated cardiomyopathy, Olson et al. focussed on finding mutations within the alpha-tropomyosin gene. Their search yielded two substitutions, which induced charge reversals of the fifth residue found in highly conserved heptad repetitive sequences (24). Consequently, electrostatic interactions between actin and tropomyosin may have been altered, precipitating local changes in tropomyosin conformation or lability (24). Alternatively, the observed mutations may have compromised the structural integrity of the protein and subsequently impeded the generation of force by the sarcomere (2;24). However, a mouse model created by Blanchard et al., using gene targeting in embryonic stem cells and blastocyst-mediated transgenesis, demonstrated that haploinsufficiency of the alpha-tropomyosin gene produced little or no change in cardiac function or structure; only a complete deficiency was incompatible with life (25). These findings imply the existence of a regulatory mechanism in heterozygotes that maintains the level of myofibrillar tropomyosin despite decreased mRNA levels (25).

Recently, mutations in the titin gene were shown by Gerull et al. to cause autosomal dominant DCM (26). A segregating 2-bp insertion mutation resulted in a frameshift and the subsequent production of a truncated protein. In addition, a missense mutation was identified and predicted to disrupt a highly conserved hydrophobic core sequence of an immunoglobulin fold in the Z-disc-I-band transition zone (26). Although

the consequences of these mutations have not been elucidated to date, the truncated titin fragment is postulated to severely affect sarcomere structure and function. Another study performed by Itoh-Satoh et al. revealed the presence of two other titin mutations at the titin-cap and alpha-actinin binding domains in Japanese DCM patients (27). These mutations caused a weaker interaction between titin and titin-cap/alpha-actinin.

In the wake of these findings, it was only a matter of time before titin-cap, the substrate of titin, became the subsequent target for further investigation. Indeed, analysis of this gene in a population of 380 DCM patients yielded a missense mutation, which led to a decreased affinity for the cysteine- and glycine-rich protein 3 (MLP) via allosteric effects on the MLP-interacting domain (28).

The same study also revealed the presence of an MLP mutation, which led to the complete loss of interaction with and subsequent mislocalization of titin-cap (28). These results support the concept that titin-cap binding to MLP is critical for maintenance of the cardiac Z disc. Mice that harbored an MLP deficiency were found to exhibit chamber dilation and contractile dysfunction (28;29). However, a detailed analysis of MLP^{-/-} papillary muscle reveals the presence of a normal recoil response, which implies that the chamber dilation is not secondary to a structural disturbance, but related to an inability to sense the mechanical stretch stimulus and to generate a primary effect on muscle tension (28). Titin has been shown to generate tension by increasing the passive stretch of cardiac muscle (28;30). All of these findings led Knöll et al. to identify the MLP/titin-cap/titin complex as a key component of the cardiomyocyte stretch sensor machinery (28). In this alternate model of DCM pathogenesis, loss of MLP would destabilize the anchoring of the Z disc to the proximal end of the titin-cap/titin complex, thereby leading

to a conformational alteration of the titin molecular spring elements. This loss of elasticity would result in the overstretching of individual myocytes and precipitate the activation of cell death pathways, through the diminished survival cues generated by the defective stretch-sensing machinery. Ultimately, progressive heart failure and DCM would ensue (28).

1.3.2 Cytoskeletal Proteins

This category of candidate DCM genes includes desmin, dystrophin, delta-sarcoglycan, and metavinculin.

Until August 1999, the cardiac actin gene was the only putative disease gene known to be responsible for the autosomal dominant form of the disease (7). However, targeted disruption of murine desmin genes had been previously shown to perturb the normal architecture of myocytes, precipitating myocyte degeneration and death (1;31). These events led to a phenotype that resembled DCM (1). Such findings prompted Li et al. to analyze desmin as a potential candidate gene for this disease. Subsequently, a missense mutation was identified as the genetic cause of DCM in a four-generation American family recruited by this team (17). However, further studies revealed that the role of desmin in the pathogenesis of DCM could only be marginal at best (7;32).

The importance of dystrophin for cardiac function was highlighted by the finding that the development of chronic DCM in Coxsackievirus B3 myocarditis resulted from the cleavage of this cytoskeletal protein via enteroviral protease 2A (12). Variants of the dystrophin gene have since been associated with an uncommon X-linked form of DCM (33). Dystrophin mutations reported to date fall into two classes: (i) those located in the promoter region or exon 1, which correlate with an absence of both dystrophin transcripts

and protein in the cardiac muscle of affected DCM patients or (ii) those found elsewhere in the gene (12;34-36).

The delta-sarcoglycan gene (SGCD) also seemed like a strong candidate for a morbid role in DCM due to a variety of reasons. First of all, it encodes a protein that is involved in the cytoarchitecture of the cardiac cell, as it is a component of the dystrophin-associated sarcoglycan complex (37). Second of all, SGCD is highly expressed in both cardiac and skeletal muscle (37). Finally, the Bio TO-2 strain of Syrian hamsters, which is one of the animal models used to represent DCM, presents with a deletion of the SGCD gene (38). The screening of this gene in a population of DCM patients revealed two mutations, which affected the secondary structure of the delta-sarcoglycan protein (9). However, further studies once again shed doubt on the significance of this gene in the pathogenesis of DCM. The prevalence of the SGCD mutations was estimated by Sylvius et al. to account for less than 1.5% of all the cases considered by both their study and the one previously conducted by Tsubata et al. (37).

Vinculin and its isoform metavinculin are protein components of intercalated discs (13). The smaller isoform, vinculin, is ubiquitously expressed. However, metavinculin is expressed exclusively in cardiac and smooth muscle. Vinculin expression has been found to be upregulated in response to mechanical loading, and targeted disruption of the gene in mice has resulted in a loss of cardiac contractility during embryonic development (39). In addition, human studies have suggested a potential relationship between metavinculin and vinculin expression, intercalated disc abnormalities and DCM (13;40). Olson et al. identified one missense mutation and one 3-bp deletion within the vinculin gene among a study population of 350 unrelated

patients with DCM (13). The mutations are each located in a different region of the vinculin tail domain and are predicted to disrupt the intricate helical organization through varying mechanisms (13). In vitro assays confirm that the metavinculin-mediated crosslinking of actin filaments is significantly altered (13). In addition, ultrastructural examination of the explanted heart tissue from one of the heterozygote patients revealed the presence of grossly abnormal intercalated discs.

1.3.3 Other Proteins Implicated in DCM

The remaining category constitutes a heterogeneous group of proteins, which are considered to be distinct from the sarcomere and cytoskeleton of the cardiac myocyte. They include tafazzin, phospholamban, and lamin A/C.

Tafazzin, also known as G4.5, is a protein of unknown function (2). A study by D'Adamo et al. linked together what were formerly considered different conditions by demonstrating that tafazzin is responsible for Barth Syndrome (OMIM 302060), X-linked endocardial fibroelastosis (OMIM 305300), and severe X-linked cardiomyopathy (OMIM 300069) (41). Barth Syndrome is a neonatal form of DCM, which is often accompanied by arrhythmias and heart failure (2).

Phospholamban (PLN) is a transmembrane phosphoprotein that inhibits the cardiac sarcoplasmic reticular Ca^{2+} -adenosine triphosphatase (SERCA2a) pump in its unphosphorylated state (42). This inhibition is relieved upon phosphorylation of the protein. This year, Schmitt et al. identified a missense mutation in the cytosolic domain of the phospholamban gene, which segregated with the affected status in a four-generation DCM family (42). Cellular and biochemical studies revealed that the mutated PLN trapped protein kinase A (PKA), which consequently blocked PKA-mediated

phosphorylation of wild-type PLN and delayed the decay of calcium transients in myocytes (42). In this way, SERCA2a was indirectly inhibited by the mutated PLN. These results indicate that myocellular calcium dysregulation can also initiate human heart failure.

Finally, the lamin A/C (LMNA) gene has also been implicated in the pathogenesis of DCM. LMNA maps to chromosome 1q21.2-1q21.3 and is 24 kbp in size (43). It comprises 12 exons, and encodes four alternatively spliced gene products: lamins A, C, Adelta10, and C2. Lamin Adelta10, a variant of lamin A in which 90 nucleotides are deleted from the 5' part of exon 10, was discovered by Machiels et al. (1996) during the RT-PCR and sequencing of cDNA from nuclear inclusions in GLC-A1 cells, a lung adenocarcinoma cell line (44). Lamin C2 is specific to the testis (45). Analysis of cDNA sequences that encode nuclear lamins reveals that they are closely related to the cytoplasmic intermediate filament protein family (46). Lamins are classified as being either A-type or B-type depending on their primary sequence, behaviour at mitosis, and tissue-specific expression patterns (47). A-type lamins are expressed exclusively in differentiated cells and tissues, whereas B-type lamins are constitutively expressed in all embryonic and somatic tissues studied to date (43;47-49). B-type lamins are also encoded by two separate genes, LMNB1 and LMNB2 (50).

Lamins are major components of the nuclear lamina. The lamina is a fibrous nucleoskeletal structure associated with the inner nuclear membrane. This inner membrane faces the chromosomes and is home to a unique set of integral proteins, such as lamin B receptor, lamina-associated peptide-1 (LAP-1), LAP-2, emerin, MAN1, otefin, Young Arrest, and nurim (49;51). Nuclear lamins interact with integral proteins

via binding sites located in their rod domains and carboxy-terminal tails (43;47;52-54). For example, an immunoglobulin-like domain extending between residues 319 and 572 of lamin A/C binds to the alpha-specific region of LAP2alpha, which is a soluble protein that mediates the expansion of reforming nuclei during the cell cycle (49;55). Furthermore, the region spanning residues 384-566 has been shown to interact with emerin, which is a type II integral nuclear protein that extends into the nucleoplasm from a transmembrane domain (54;56). Studies have shown that emerin and lamin A are colocalized in various heart and kidney cell types (56). In addition, Clements et al. was able to demonstrate a direct interaction between recombinant emerin and lamin A using biomolecular interaction analysis and monoclonal antibodies (56).

However, lamins are not restricted to the nuclear periphery (57;58). Studies have shown that A-type and B-type lamins may be found within the nucleus as distinct nucleoplasmic foci (58;61). In addition, A-type lamins may form part of a diffuse intranuclear network (57). A-type lamin foci have been observed during lamina assembly (59), are most prominent during the G1 phase of the cell cycle, and are closely associated with condensed chromatin (48). These lamin speckles were also shown to colocalize with RNA splicing factors compartments (141). On the other hand, B-type lamin foci are predominantly found during S-phase in association with DNA replication centres and do not colocalize with lamin A spots (58). The exact function of these various types of intranuclear speckles, and whether they are general or cell type-specific phenomena, remains to be established (48). However, it has been suggested that A-type lamin speckles may form part of a dynamic structure that can be rapidly modulated by

specific signaling events to spatially organize mRNA splicing and pol II transcription (141).

1.4 Lamin Function

Nuclear lamins are extremely versatile proteins. In addition to playing key structural roles, such as maintaining the integrity of the nuclear architecture and providing anchorage sites for chromatin, nuclear lamins are also involved in DNA replication, RNA pol II transcription and signal transduction.

1.4.1 Nuclear Organization

Functional studies confirm the importance of A-type lamins in maintaining the integrity of the nuclear architecture. Partial deletion of the LMNA gene in mouse embryonic fibroblasts (MEFs) produced nuclei that were often highly elongated or irregular (62). Although the nuclei remained intact, the overall impression is of large-scale herniation of the nuclear membranes (62). At the ultrastructural level, cells derived from LMNA^{-/-} mice exhibited striking abnormalities, such as the withdrawal of B-type lamins, LAPs and nuclear pore complexes (NPCs) from one pole of the nucleus (52). In addition, emerin is inefficiently retained at the nuclear periphery and partially mislocalized to the peripheral endoplasmic reticulum (52). This evidence strongly supports a role for A-type lamins in the correct localization of emerin. However, emerin is not uniformly lost in tissues from LMNA null mice, which may suggest the involvement of additional factors (62). Nuclei assembled in vitro under lamin-depleted conditions are also rather fragile and easily broken (49). Taken together, these results

clearly indicate that A-type lamins play an essential role in the nuclear organization of differentiated cells.

1.4.2 Anchorage Sites for Chromatin

Recent work from several labs has demonstrated that the lamina is of fundamental importance, not only in maintaining the structural integrity of the nuclear envelope, but also in organizing chromatin within the nucleus. Cytological studies show that a large proportion of condensed chromatin borders the inner nuclear membrane, and that proximity to this membrane helps to repress partially silenced genes (55). Ultrastructural examination of LMNA^{-/-} MEFs and hepatocytes revealed a thinning or loss of heterochromatin at discrete regions of the inner nuclear membrane (62). These segments of the nuclear envelope, which also lack morphologically identifiable NPCs, likely correspond to the herniations observed in the light microscope (62).

Although their functions in nondividing cells such as cardiac myocytes are largely unknown, lamins A and C contain a chromatin-binding site and may participate in ordering the higher structure of the genome (55). A number of biochemical studies have suggested that lamin tail and rod domains can bind directly to DNA, chromatin, and core histones (63-66). More recent work has suggested that lamin A might make indirect interactions with the chromatin through a chain of interactions involving the LEM family proteins, such as emerin and LAP2 (63). The LEM domain consists of a helical turn, followed by two helices separated by a 12-residue loop (50). LAP2 is unique among known LEM proteins in possessing both a DNA-binding LEM-like domain and a BAF-binding LEM domain (50). BAF (barrier to autointegration factor) is a highly conserved, small dimeric DNA-binding protein (49). In vitro, BAF crossbridges DNA molecules

and colocalizes with chromatin throughout interphase and mitosis (49). Although BAF is postulated to play a fundamental role in the chromosome architecture of complex eukaryotes, its function *in vivo* remains obscure (49). However, it was demonstrated by Zheng et al. (2000) that elimination of BAF by RNAi in *C. elegans* gives rise to chromosomal segregation defects (67). The interaction of lamins with these LEM family proteins, as well as BAF-1 and HP1 chromodomain proteins, may provide anchorage sites for chromatin fibers at the nuclear periphery (68). Lamins may also bind to “soluble proteins” that associate with the chromatin, such as Young Arrest (YA) and the tumour-suppressor Rb (49). YA is found in *Drosophila* embryos, where it mediates the transition from meiosis to mitosis and has affinity for decondensed chromatin (49). Rb is a central regulator of the cell cycle and inhibits genes required for S phase by recruiting histone deacetylases that generate repressive chromatin structures (69). It binds specifically to both A-type lamins and is concentrated at the lamina of the nuclear envelope (49). These findings indicate that not only do A-type lamins provide anchorage sites for chromatin, either directly or indirectly, but that they may also play a role in the regulation of gene expression (70).

1.4.3 DNA Replication

The most dramatic alterations in lamin organization take place during mitosis in more complex cells, when disassembly of the nuclear envelope must occur in order for the condensed chromosomes to access the mitotic spindle (57;71). Disassembly of the nuclear lamina is initiated by phosphorylation of the serine and threonine residues at either end of the coiled-coil domain (71-73). During this process, lamins A and C are rapidly released throughout the nucleoplasm in early prophase while lamin B remains at

the nuclear periphery until prometaphase (57). Another study performed by Moir et al. also emphasized the importance of lamin organization in facilitating DNA replication (74). Dominant negative lamin mutants lacking their N-terminal domains were added to assembled nuclei in *Xenopus* extracts (74). Disruption of lamin organization in this manner prevented the resumption of DNA replication after the release of AraC, a reversible inhibitor that blocks near the onset of the elongation phase (74). Additionally, intranucleoplasmic lamin structures have been reported in association with DNA replication centres in S phase cells (58;60). These foci could be detected by antibodies against lamin B; however, the nuclear staining patterns obtained with antibodies directed against A-type lamins in mid-late S phase cells did not coalign with these lamin B-containing structures (58). This implies a role for lamin B also exists in the organization of replicating chromatin during S phase.

1.4.4 RNA Polymerase II Transcription

In a twist on the study conducted by Moir et al., Spann and colleagues performed another experiment in which dominant negative lamin mutants lacking the N-terminal domain were used to disrupt the normal organization of the nuclear lamina (75). Consequently, RNA pol II activity in both mammalian cells and transcriptionally active embryonic nuclei from *Xenopus laevis* was inhibited in a highly specific manner (75). Immunofluorescence observations indicate that this selective inhibition of pol II-dependent transcription involves the TATA binding protein, a component of basal transcription factor, TFIID (75). The fact that activities of certain other transcription factors, such as Rb, Oct1, Pdx1, and GCL, include interactions with the lamina also suggests that lamins play an active role in transcriptional repression (45;55).

1.4.5 Signal Transduction

In non-dividing cells such as cardiac myocytes, lamins may participate in signal transduction by mediating molecular movement between the cytoplasm and the nucleus (76). Martelli et al. demonstrated that lamin A binds to the CalB domain of protein kinase C (PKC) at a site downstream of residue 499 in its carboxy-terminus (77). PKC is a serine/threonine protein kinase and is part of a family of enzymes that occupies critical nodes in the complex signal transduction networks, which regulate diverse cellular processes such as gene expression, proliferation, apoptosis, and hypertrophy (77). Lamin phosphorylation by PKC has been linked with both cell proliferation and apoptosis (77-79). Aberrations in signaling pathways regulating cell proliferation and apoptosis are strongly connected with developmental abnormalities as well as a variety of chronic disorders, and may prove to be a mechanism by which lamin mutations mediate the pathogenesis of DCM, among other diseases (77).

1.5 Lamin Mutations and Disease

Not only are lamins known to possess many different roles within a cell, they are also postulated to be a causative factor in numerous diseases. To date, seven different disorders have been linked to mutations in the lamin A/C gene. Despite marked differences in the predominant clinical phenotypes of these diseases, cardiac disease is often a common manifestation of these allelic disorders.

1.5.1 Emery-Dreifuss Muscular Dystrophy (EDMD)

EDMD was first described in 1966 by Alan Emery and can typically be defined by three main clinical features (49;80;81). First, there are early contractures of the

Achilles tendons, elbows, and posterior cervical muscles, with initial limitation of neck flexion progressing to restricted forward flexion of the entire spine (81). Second, slowly progressive muscle wasting and weakness with a humeroperoneal distribution occurs early in the course of the disease (81). Wasting is usually more severe in specific muscles of the lower leg, upper arm and shoulders, but other muscles may show myopathic features histologically (80). Smooth muscle function is unaffected (80). Third, cardiac involvement becomes more evident as muscle weakness progresses, and is usually present by 30 years of age (80). The initial manifestation consists of conduction defects, although ventricular dysrhythmias and dilated cardiomyopathy may also arise (54). By the third or fourth decade of life, affected individuals invariably develop heart block or severe dysrhythmias that may require a pacemaker or an implantable defibrillator (43;53;54). However, EDMD is characterized by variable expressivity of the phenotype. In other words, individuals within the same family may be affected to varying degrees, and some members may display no symptoms at all (80).

EDMD was initially described as an X-linked disorder, although autosomal dominant and recessive forms were also later reported (82). The X-linked form is caused by mutations of the STA gene at Xq28. This gene was later found by Bione et al. to encode a transmembrane protein expressed in virtually all somatic cells that was subsequently named “emerin” (70). Four years later, Bonne et al. mapped the locus for autosomal EDMD to the LMNA gene, and identified the first four mutations associated with this form of the disease (53). In 2000, Felice et al. described two other mutations that were located within the rod domain of lamin A/C (83). That same year, Bonne et al. expanded upon their previous work by discovering twelve novel mutations in another

EDMD population scattered throughout exons 1 to 9 of the LMNA gene (54). This study highlighted the fact that substantial interfamilial variability exists between carriers of the same mutation and revealed the possibility that modifier genes may play a significant role in determining the course of this disease (54). Di Barletta et al. further extended the mutation analysis with the description of a 1 bp-deletion and five additional missense mutations (82). Unlike all the other substitutions that had been reported up to that time, H222Y occurred as a homozygous mutation, and was found in a patient who presented with a severe form of muscular dystrophy without any cardiac symptoms (82). This was later believed to represent the first case of an autosomal recessive form of EDMD.

The functional consequences of these lamin A/C mutations were elucidated to some degree by various studies. Markiewicz et al. analyzed fibroblasts from X-linked EDMD patients and noted that all lamin subtypes appeared to possess increased solubility properties compared to normal individuals (84). In addition, lamin C and LAP2alpha were mislocalized in these fibroblasts (84). Electron microscopy of cells and tissues from EDMD patients has revealed the presence of disruptions at the nuclear rim and changes in heterochromatin distribution (80;85), similar to the nuclear alterations that were observed in over 80% of the embryonic fibroblasts from LMNA^{-/-} mice (62). Thus, it appears that, at the very least, the structural integrity of the nucleus is compromised by LMNA mutations found in EDMD patients.

1.5.2 Limb Girdle Muscular Dystrophy (LGMD)

As can be inferred by its name, LGMD encompasses another clinically and genetically heterogeneous group of myogenic disorders with a limb-girdle distribution of muscle weakness (86). To date, four dominant and eight recessive forms have been

identified. The majority of LGMD cases are characterized by the autosomal recessive transmission of mutations found mainly in the sarcoglycan gene, and elevated phosphocreatine kinase levels (9). LGMD was first described as an autosomal dominant trait (LGMD1B) by van der Kooi et al. (9). Like EDMD, the disorder is slowly progressive with age-related atrioventricular cardiac conduction disturbances and DCM; however, there is an absence of early contractures (86).

Muchir et al. described three novel LMNA mutations within a population of LGMD1B patients (86). Two of these mutations were found within the central rod domain that is implicated in the dimerization of lamins, while the third resulted in the production of a truncated protein, which lacks half the C-terminal globular tail domain (86). Ki et al. also reported a substitution at codon 377, but to leucine instead of histidine (87). This particular residue is located within a region of 32 amino acids that is highly conserved in all intermediate filaments at the end of the rod domain (86). By a systematic mutagenesis of this region, Heald et al. demonstrated that the R377H mutation abolishes the assembly of normal nuclear lamina (86). In addition, transfection of lamins with C-terminal truncations into CHO cells produced structural alterations of both the nuclear envelope and the nucleus. This finding suggests that the pathogenic mechanism of the splice donor site mutation may also involve perturbation of the nuclear architecture (86).

1.5.3 Dunnigan-Type Familial Partial Lipodystrophy

Lipodystrophies are rare disorders characterized by the selective but variable loss of adipose tissue (88). There are two major types of lipodystrophies: familial or acquired (88). Dunnigan-type familial partial lipodystrophy is an autosomal dominant disorder

(88). Affected patients are born with normal fat distribution, but develop muscular hypertrophy and begin to lose subcutaneous adipose tissue from the extremities, trunk and gluteal region with the onset of puberty (89). Excess fat may also be deposited in the face, neck, back, labia majora, and intraabdominal region (89-91). However, intermuscular, intraabdominal, intrathoracic, and bone marrow adipocyte stores remain normal (89). In young adulthood, patients develop hyperlipidemia and insulin-resistant diabetes. Most will characteristically die of cardiovascular complications by 40-60 years. The morphotype in men is less typical and usually appears late (92).

In 1998, the genetic locus for this disease was mapped to chromosome 1q21-q22 (70;93). Two years later, Cao and Hegele proposed that LMNA might be a candidate for Dunnigan-type partial lipodystrophy because the regional muscle wasting observed in EDMD could be analogous to the regional adipocyte degeneration that occurs in this condition (89). DNA sequencing of LMNA in five Canadian familial partial lipodystrophy (FPLD) probands indicated that each had a novel missense mutation, which co-segregated with the disease phenotype and was absent in 2000 normal alleles (89). Heterozygotes were observed to possess significantly higher levels of triglycerides, insulin and C-peptide, but significantly lower levels of HDL cholesterol (94). Functionally, this mutation was found by Hegele et al. to reduce plasma leptin levels (95). However, it did not have an effect on the interaction of lamin A with emerin or its targeting to the nucleus (96). Two other substitutions were identified in FPLD patients at this codon (43;90;97;98). Further studies extended the mutation analysis to two more codons within exon 8 (43;91). Then, Speckman et al. reported a mutation within exon 11 in a patient with lipotrophic diabetes (90). Although two copies of this mutant allele

must be inherited in order for the disease to occur, this was the first indication that a mutation solely within lamin A could also be capable of causing FPLD (70). Shortly after, both Hegele and Vigouroux et al. discovered yet another missense mutation within exon 11 (97;98). Together, these findings indicate that a spectrum of LMNA mutations underlies FPLD and that aberrant lamin A is more likely than lamin C to play a role in the pathogenesis of this disease.

1.5.4 Charcot-Marie-Tooth Disorder Type 2 (CMT2)

CMT constitutes a genetically heterogeneous group of inherited motor and sensory peripheral neuropathies, which are mainly characterized by muscle weakness and wasting, foot deformities, and electrophysiological, as well as histological, changes (99;100). The most frequent mode of inheritance appears to be autosomal dominant, reported in both the demyelinating and axonal forms of CMT, but in some areas (ex. Algeria, where consanguineous marriages are found in 23% of the population), it seems that the recessive forms are more frequent (99). CMT2 is characterized by axonal degeneration of peripheral nerves (70). Homozygosity mapping in consanguineous families with autosomal recessive CMT2 provided evidence of linkage to chromosome 1q21.2-q21.3 in two families (100;101). A specific LMNA missense mutation, located in the lamin A/C rod domain, was subsequently found in all affected members of these families and in other unrelated CMT2 patients (100).

1.5.5 Mandibuloacral Dysplasia (MAD)

MAD is a rare autosomal recessive disorder, characterized by postnatal growth retardation, craniofacial anomalies, skeletal malformations, and mottled cutaneous pigmentation (102). Patients display loss of subcutaneous fat in the extremities and the

accumulation of adipose tissue in the trunk, face, submental region (underneath the chin), and occiput (back of the head or skull) (102). Since patients with MAD frequently have partial lipodystrophy and insulin resistance (45), Novelli et al. hypothesized that the disease may be caused by mutations in the LMNA gene (102). Screening of five consanguineous families with MAD identified the presence of a LMNA missense mutation in affected individuals (102). Patient fibroblasts contained nuclei that presented an abnormal “honeycomb” distribution of lamin A/C and a dysmorphic nuclear envelope (102). Interestingly, a binding site for the adipocyte-differentiation factor sterol-response element-binding protein 1 (SREBP1) was identified on lamin A between residues 227 and 487 (102). This argues for the possibility that the fat loss observed in FPLD and MAD may be caused by reduced binding of SREBP1 to lamin A (102).

1.5.6 Hutchinson-Gilford Progeria Syndrome (HGPS)

HGPS is a rare genetic disorder resulting in phenotypes that are suggestive of accelerated aging (45). Children affected with HGPS typically appear normal at birth, but within one year, the characteristic features of failure to thrive, delayed dentition, alopecia, and sclerodermatous skin changes begin to appear (103). Death occurs on average at around 13 years of age, and at least 90% of these patients succumb to progressive atherosclerosis of the coronary and cerebrovascular arteries (103). The HGPS gene was recently localized to chromosome 1q (103). Three LMNA coding sequence variants were identified in seven unrelated HGPS probands earlier this year by Cao and Hegele (104). Soon after, De Sandre-Giovannoli reported the discovery of a de novo LMNA substitution in two unrelated HGPS patients (105). Although this mutation had no effect on the translated amino acid, it was found to activate a cryptic splice site

within exon 11, which resulted in the production of a truncated lamin A protein (105). Western blotting showed that the carriers of this mutation expressed only 25% of normal lamin A levels, whereas no truncated form was detected (105). This same mutation was rediscovered by Eriksson et al. shortly thereafter in 18 out of 20 classical cases of HGPS (103). One additional subject was identified with a different substitution at the same codon, which also activated a cryptic splice site within exon 11 and produced a truncated protein (103). The deleted region at the C-terminus was predicted to contain sites required for endoproteolytic cleavage of prelamin A and phosphorylation during certain phases of the cell cycle (103).

1.5.7 Dilated Cardiomyopathy (DCM)

Last, but certainly not least, lamin A/C mutations have also been implicated in the pathogenesis of DCM – in fact, more so than any other gene by research teams across the world. However, the findings that have been accumulated to date must be interpreted in light of the limitations that are an inherent part of this research. This includes the fact that most of the genes associated with DCM have been found using a candidate gene strategy rather than positional cloning. Other complications include the incomplete penetrance of this disease, which renders it extremely difficult to ascertain the causality of reported mutations. In addition, all of the putative DCM-causing genes have also been implicated in at least one other disease, with the exception of metavinculin.

This study focuses on the role of the lamin A/C gene in DCM for several reasons. First of all, three of the Polish families recruited for our study had DCM with conduction system disease and high phosphocreatine kinase levels. In addition, one of the Canadian families had a history of muscular dystrophy with severe cases of early onset DCM.

These observations seemed to point directly at LMNA as the putative disease-causing gene in a significant proportion of our patient population.

Despite the series of novel missense LMNA mutations that have been discovered in DCM patients since 1999, surprisingly few studies have focussed on the functional consequences of these genetic variants. It is evident that further research must be performed in order to elucidate the etiology of this disease. Therefore, one of the aims of this study is to determine the existence or degree of potential ultrastructural and lamin A/C mRNA abnormalities in the cardiac tissue of DCM patients. This will be accomplished by screening DCM patients for LMNA mutations through the analysis of DNA extracted from blood samples via single strand conformation polymorphism (SSCP) and/or denaturing high performance liquid chromatography (DHPLC), followed by the automated sequencing of abnormal profiles. The functional consequences of these mutations will subsequently be assessed through the examination of cardiac tissue samples from end-stage DCM patients via electron microscopy. In addition, the expression levels of wild-type and mutated LMNA mRNA will be analyzed using quantitative RT-PCR and restriction fragment length polymorphism (RFLP) assays.

1.6 Statement of Objectives

The main objectives of this study are two-fold:

1. To identify novel mutations in the LMNA gene that may predispose individuals to DCM
2. To determine the relative expression levels of wild-type vs. mutated LMNA mRNA in the cardiac tissue of end-stage DCM patients.

2 MATERIALS AND METHODS

2.1 Patient Population

All patients were recruited as part of the study population, or as controls, with their informed and written consent. The assessment of idiopathic dilated cardiomyopathy was based on strict diagnostic criteria, delineated by the WHO/ISFC and modified according to Mestroni et al. (106). Major criteria included the presence of: i) depressed left ventricular systolic function, as indicated by an echocardiographic, radionuclide scanning, or angiographic ejection fraction $<45\%$; ii) left ventricular dilatation, as determined by the presence of an end-diastolic diameter $>117\%$ of the predicted value, corrected for age and body surface area as described by Henry et al. (107). Minor criteria consisted of: i) unexplained supraventricular or ventricular arrhythmias (frequent, $>1000/\text{day}$, or repetitive, $>120/\text{min.}$) before the age of 50; ii) left ventricular dilatation $>112\%$ of the predicted value; iii) left ventricular dysfunction, as defined by an ejection fraction $<50\%$; iv) unexplained conduction disease, including type II or III atrioventricular conduction defects, complete left bundle branch block, and sinus nodal dysfunction; v) family history of an unexplained sudden death or stroke before 50 years of age.

Exclusion criteria were based on those described by Michels et al (108) and include: non-Caucasian origin, sustained systemic arterial hypertension (defined by documented and confirmed blood pressure readings $>160/110$ mmHg at repeated intervals and/or evidence of target-organ disease), coronary heart disease (obstruction $>50\%$ of the luminal diameter in a major branch), myocardial infarction, history of

chronic excess of alcohol consumption (>40 g/day for females and >80 g/day for males over a period of more than 5 years, according to WHO criteria (109)) with remission of dilated cardiomyopathy after 6 months of abstinence, persistent high rate supraventricular arrhythmias, pericardial or congenital heart disease, cor pulmonale, hyperthyroidism, insulin-dependent diabetes, hemochromatosis, and systemic diseases.

All patients and first-degree relatives were evaluated by history, physical examination, and electrocardiography, as well as by M-mode and cross-sectional echocardiography. The clinical status of the relatives of each index case was subsequently determined according to the following strategy:

1. Affected, in the presence of the major criteria, isolated left ventricular dilation and another minor criterion, or 3 minor criteria
2. Uncertain, in the presence of 1 or 2 minor criteria
3. Unaffected, in all other cases.

2.2 Tissue Collection

In the event that any of the patients from our study population were placed on the University of Ottawa Heart Institute transplant list, written and informed consent was obtained to collect tissue from the explanted heart. Samples measuring 2 cm by 2 cm were excised from all four chambers of the heart, i.e. the left and right ventricles and atria, and immediately frozen in liquid nitrogen. The explanted heart tissue samples were then stored at -80°C.

2.3 DNA Extraction

After receiving informed and written consent, three 7 mL blood samples were collected in sterile vacutainer tubes containing EDTA from patients and their first-degree relatives. DNA was extracted from the buffy coat of the whole blood using standard procedures described by Miller et al. (110).

2.4 Genomic DNA Amplification

The entire LMNA coding region was amplified by polymerase chain reaction (PCR). For the most part, oligonucleotide primers were derived from the published sequences of introns flanking each of the twelve LMNA exons (Genbank accession number: L123399 [exon 1], L12400 [exon 2], and L12401 [exon 3-12]). However, exons 1 and 11 were amplified in sets of two overlapping fragments, consisting of 209 bp and 352 bp for exon 1, and 276 bp and 178 bp for exon 11 (Appendix II). Primers for exons 1, 5, and 11 were designed using Oligo software. All other primer sequences were obtained from <http://genetics.med.harvard.edu/~seidman/primersequence.html> (Appendix II). PCR was performed in a 25 μ l reaction volume containing 50-96 ng of genomic DNA, 0.25 U taq polymerase (Qiagen), 0.8 μ M of each primer, 200 μ M dNTPs (Invitrogen), 1.5 mM MgCl₂, 20 mM Tris-HCl (pH 8.4), 50 mM KCl, and 5 μ l of solution Q (Qiagen). The PCR program consisted of an initial denaturation step at 94°C for 5 min., followed by 30 cycles of amplification (denaturation at 94°C, annealing at 50-65°C [see Appendix II], and extension at 72°C for 1 min. each) and a final elongation period at 72°C for 10 min.

2.5 Single Strand Conformation Polymorphism (SSCP)

SSCP was used to screen for mutations in the resulting PCR products according to the protocol described in Tesson et al. (7). Briefly, 2 μ l of the PCR product was denatured at 95°C for 5 minutes and then separated on a 10 % polyacrylamide (40% acrylamide/bis acrylamide solution, 37.5 :1) mini-gel at 10°C and 20°C. Electrophoresis was performed at 8-12 mA using an OWL Penguin apparatus. The resultant DNA bands were visualized with a DNA silver staining kit (Amersham Pharmacia Biotech AB). Polyacrylamide gels were subsequently laminated using a GelAir dryer (Bio-Rad) for photodocumentation and long-term storage.

2.6 Denaturing High Performance Liquid Chromatography (DHPLC)

PCR amplicons from the LMNA gene were also screened for mutations via DHPLC (Varian). Both buffer A (0.1% triethylammonium acetate [TEAA], 0.025% acetonitrile [ACN], pH 7), and buffer B (0.1% TEAA, 25% ACN, pH7) were used at a flow rate of 0.45 ml/min. Half of each PCR product was mixed with an equal amount of a previously sequenced and confirmed wild-type DNA. Mixed and unmixed samples were then denatured at 95°C for 3 min. and gradually cooled to 65°C at a rate of 1°C/min. to allow for the formation of heteroduplexes. The optimal partial denaturing column temperature was predicted by entering the sequence in the Stanford Melt Program found at <http://insertion.stanford.edu/meltdoc.html>. These temperatures were further optimized by determining the retention time (t_r) of each fragment. The chosen temperatures

correspond to the point at which the retention time was 75% of ($t_{r,max} - t_{r,min}$) (see Appendix III).

2.7 DNA Sequencing

All PCR samples displaying aberrant SSCP and/or DHPLC profiles compared to wild-type controls were sequenced using the ABI Prism 310 Genetic Analyzer (Applied Biosystems). An initial PCR reaction was performed with the Big Dye™ Terminator Cycle Sequencing Ready Reaction (Applied Biosystems) to incorporate fluorescent dideoxynucleotides into the DNA. Prior to sequencing, DNA samples were purified using the DyeEx™ Spin Kit (Qiagen), dried on a heating block at 95°C for 10 minutes, resuspended in 25 µl deionized formamide, and denatured at 95°C for 5 minutes. DNA sequencing was then performed in both directions, initiated separately by the forward and the reverse primers described in Appendix I.

2.8 Electron Microscopy

Tissue samples from the explanted hearts were fixed in 1.6 % gluteraldehyde and processed into thick and thin sections, according to standard methods. Tissue sections were examined with a Hitachi 7100 electron microscope.

2.9 RNA Extraction

Flash-frozen, explanted heart tissue samples were disrupted with a mortar and pestle under liquid nitrogen and homogenized using QIAshredder columns (Qiagen). The RNeasy Mini Kit (Qiagen) was used in conjunction with the RNase-Free DNase Set

(Qiagen) to extract total RNA. Extracted RNA was quantified by total absorbance at 260/280 nm and sample quality was confirmed by agarose gel electrophoresis.

2.10 Quantitative RT-PCR

First-strand cDNA was synthesized by incubating 1 µg total RNA with 50 ng oligo(dT)₁₂₋₁₈ primer (Invitrogen) at 65°C for 10 min. After a brief cooling step on ice, 1X Expand reverse transcriptase buffer (50 mM Tris-HCl, 40 mM KCl, 5 mM MgCl₂, 0.5% Tween 20 (v/v), pH 8.3) (Roche), 10 mM DTT (Roche), 1 mM of each dNTP (Invitrogen), and 50 U Expand Reverse Transcriptase (Roche) were added to each sample for a final volume of 20 µl and incubated at 42°C for 1 hour.

Quantitative RT-PCR of the resultant cDNA was performed on the LightCycler instrument (Roche) using SYBR Green I dye (Roche). Standard curves, consisting of six different dilutions (100, 50, 10, 1, 0.1, and 0.01 pg/µl), were generated in duplicate for both LMNA and the housekeeping gene, GAPDH. The pEYFP-C1 vector (Clontech Laboratories) containing a LMNA mRNA insert between EcoRI and BamHI restriction sites and the pCR[®] 2.1-TOPO[®] vector (Invitrogen) containing a GAPDH insert (provided by A. Gauthier), produced through the amplification of the GAPDH gene using the primers described below and constructed according to the TOPO TA cloning kit (Invitrogen), were used to create these standard dilution curves.

For each sample, the amounts of LMNA cDNA and GAPDH were determined. The primers for LMNA were 5'-GTGTGGAAGGCACAGAACACCT-3' (forward) and 5'-GCGGATCCTCAGCGGCGGCTACCACTCA -3' (reverse). Primer sequences for GAPDH were 5'-GTCGGAGTCAACGGAT-3' (forward) and 5'-

CCACGACGTACTCAGC-3' (reverse). The ratio of LMNA-to-GAPDH was calculated as the normalized value. The PCR mixture for both LMNA and GAPDH consisted of 11.7 μ l water, 0.8 μ l (2 mM) $MgCl_2$, 0.5 μ l (0.5 μ M) primers, 2 μ l LightCycler Fast Start DNA Master SYBR Green I and 5 μ l of a 1:5 dilution of cDNA. Cycling conditions consisted of an initial denaturation step at 95°C for 10 minutes, subsequently followed by 50 cycles of denaturation at 95°C, annealing at 58°C, and extension at 72°C for 15 seconds each. The temperature transition rate was set at 20°C/s. RT-PCR products were then analyzed by electrophoresis on a 1% agarose gel stained with 0.2 M ethidium bromide.

2.11 Restriction Fragment Length Polymorphism (RFLP) Analysis

RFLP analysis was accomplished by digesting 5 μ l of PCR products from the amplification of LMNA cDNA with 1 U *HinP1I* (New England Biolabs) for 1 hour at 37°C in a final volume of 50 μ l. Digested fragments were visualized on a 4% agarose gel stained with 0.2 M ethidium bromide. Band intensities were quantified using Quantity One software.

3 RESULTS

3.1 Identification of Novel LMNA Mutations in DCM Patients

To date, 233 DCM patients have been recruited with 119 Caucasian non-affected individuals as wild-type controls for the verification of mutations. From this study population, 108 subjects, comprising 11 familial and 81 sporadic cases, were thoroughly analyzed for mutations within the LMNA gene through an initial screening process with SSCP and/or DHPLC, followed by automated DNA sequencing in the presence of an aberrant profile. In all, four LMNA mutations were identified in four unrelated patients through this procedure. Heart tissue was obtained from two of these individuals. As a result, the following experiments and findings are focused mainly on these two subjects.

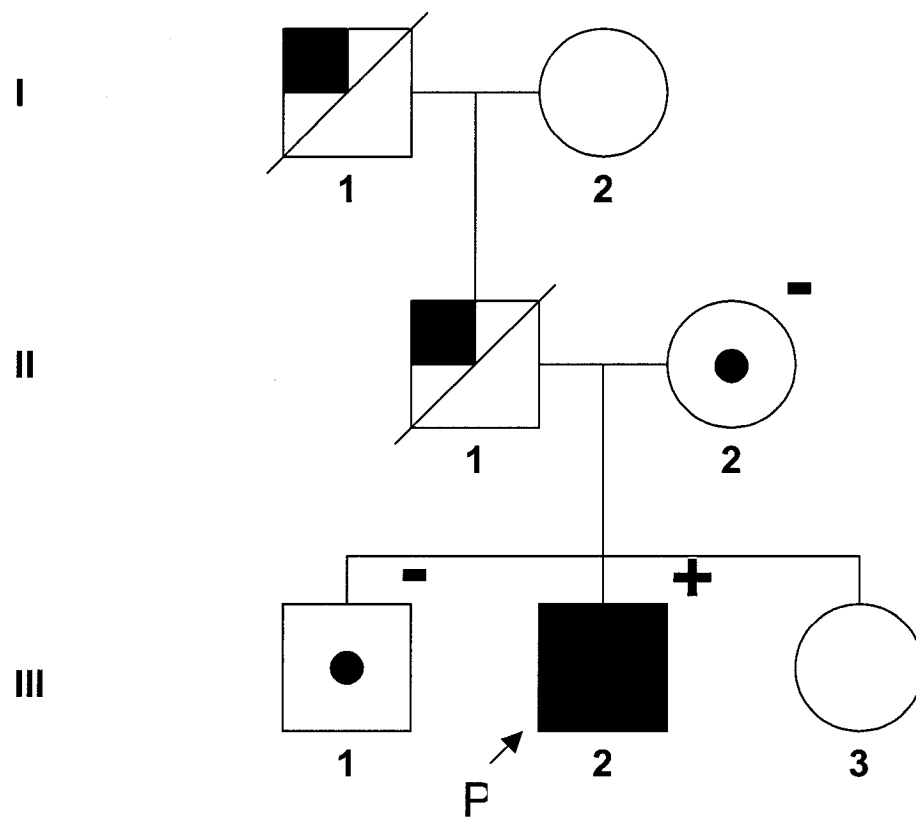
3.1.1 Patient 1

3.1.1.1 Family History

The family of Patient 1 was recruited from Poland and consisted of 3 living generations. A partial pedigree depicting the affected individuals is shown in Fig. 1. Both the proband's father (II-1) and paternal grandfather (I-1) died of heart failure at relatively early ages (37 and 42 years, respectively) which suggests that the DCM may have been transmitted in an autosomal dominant manner. The proband was a 27-year-old patient with a one year history of progressive heart failure and mild conduction system disease (first degree atrioventricular block [PR = 0.22s] and intraventricular conduction delay [QRS complex duration of 124 ms]). Clinical evaluation with a Doppler two-dimensional echocardiogram revealed the presence of a mildly dilated left ventricle (left

Fig. 1. Partial Pedigree of Patient 1.

Squares indicate males; circles indicate females. Symbols with diagonal slashes represent deceased subjects. The proband is indicated by an arrow. Individuals affected with DCM are shaded in black. Blue circles represent the individuals from which DNA samples were obtained. Symbols with red squares correspond to individuals who have undergone heart failure. (+) and (-) indicates the presence or absence of the LMNA D192G mutation in the DNA samples of family members who were screened by PCR/DHPLC/sequencing.



ventricular end-diastolic dimension of 3.4 cm/m²) with profound diffuse hypokinesis, moderate mitral and tricuspid regurgitation, as well as severe pulmonary hypertension. However, results from a coronary angiography and creatine phosphokinase (CPK) levels were normal. There were also no indications of skeletal muscle disease. One year after his diagnosis, the proband died of refractory heart failure. Biopsies of his heart were assessed by electron microscopy and immunohistochemistry. DNA samples were also obtained from the proband (III-2), as well as his mother (II-2) and 25-year-old brother (III-1). Each exon of the LMNA gene was amplified using PCR and subsequently screened for mutations via DHPLC.

3.1.1.2 Mutation Analysis

An abnormal DHPLC elution profile was observed for Patient 1 (III-2) during the analysis of LMNA exon 3 (Fig. 2). DNA sequencing revealed heterozygosity for a single nucleotide transition from A→G in codon 192, resulting in an aspartic acid to glycine substitution (Fig. 3). This mutation was not present in 200 control chromosomes obtained from a random sample of healthy individuals or other non-affected members of the family, as assessed through screening by DHPLC (data not shown; Fig.1). The affected amino acid is located in coil 1b of the central alpha-helical rod domain, which is highly conserved among various species (Fig. 4).

Fig. 2. DHPLC Analysis of LMNA exon 3 in Patient 1 and Control Samples.

DNA extracted from Patient 1 and 108 other individuals from the study population was screened for LMNA mutations through amplification with PCR followed by DHPLC. An abnormal elution profile was obtained for Patient 1 during the screening of LMNA exon 3, as compared to the control subjects.

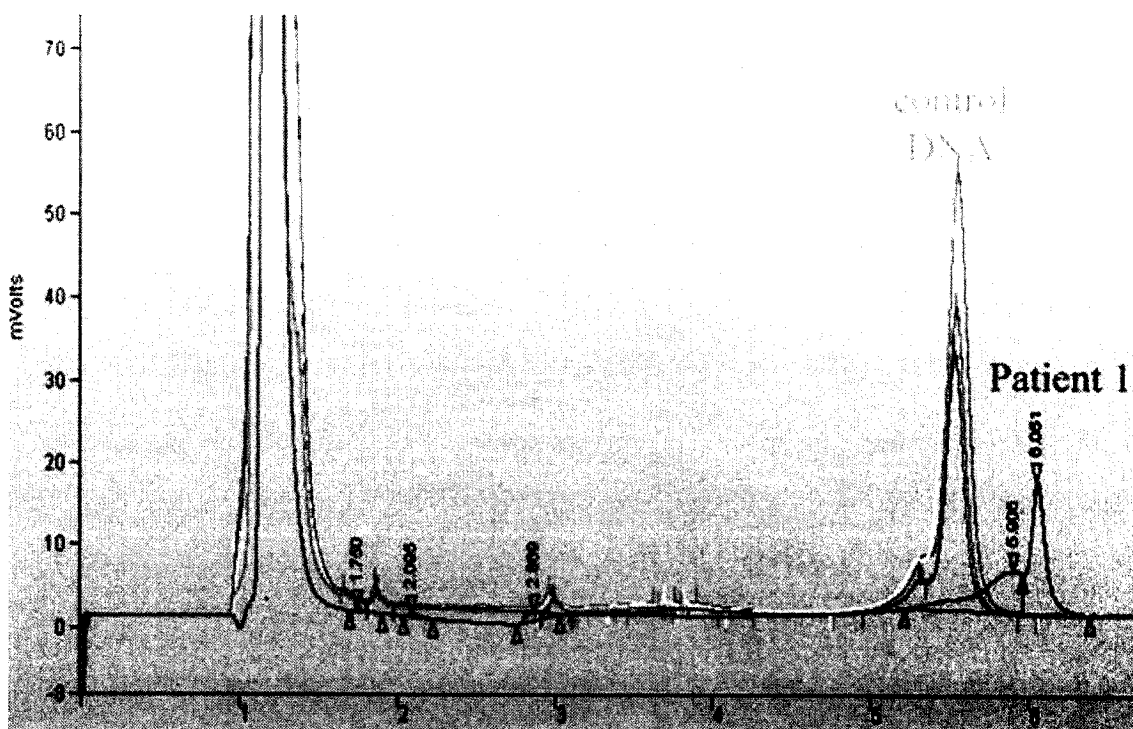
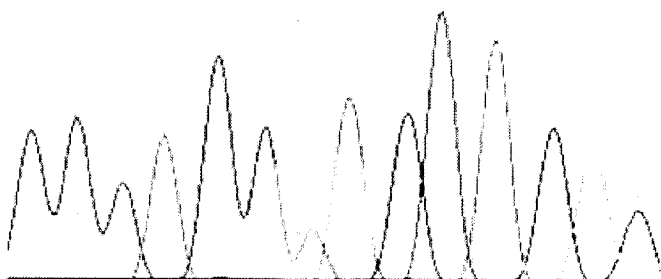


Fig. 3. DNA Sequencing Electropherograms of LMNA exon 3 from Patient 1 and Control DNA

Highlighted area indicates the position of the A→G transition, which leads to a substitution of the wild-type aspartic acid (GAT) by glycine (GGT) at codon 192 (D192G). Patient 1 is heterozygous for the D192G mutation.

Patient 1

90
G G G T G G G T G C T G A G
A → G

**Control**

90 100
G G G T G G G T G C T G A G

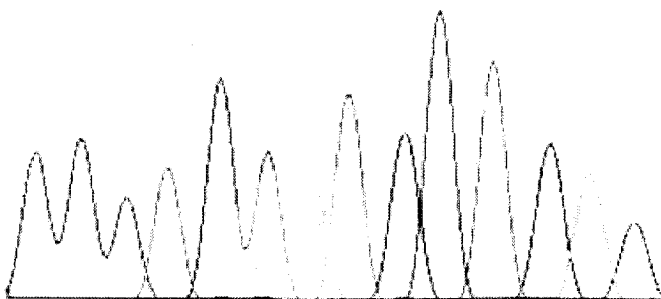
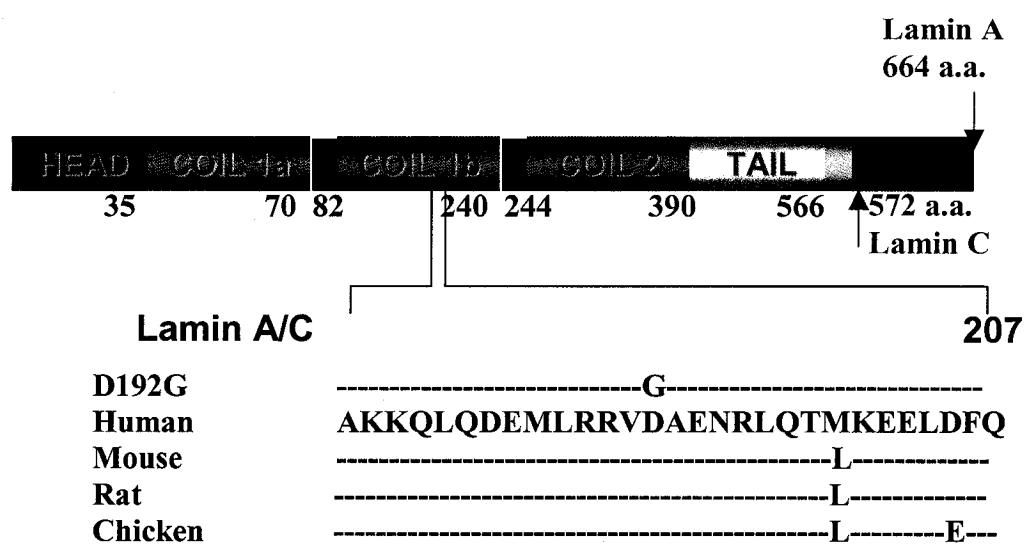


Fig. 4. Location of the D192G Mutation Within the Secondary Structure of Human LMNA.

The affected amino acid is located in coil 1b of the central alpha-helical rod domain, which is highly conserved among various species. The position of the mutated residue is highlighted in yellow.



3.1.2 Patient 2

3.1.2.1 Family History

The family of Patient 2 was recruited from Halifax and consisted of five generations in total. A partial pedigree, which includes all of the affected individuals, is shown in Fig. 5. Five different members of this family were fully screened (III-2, IV-1, V-1, V-2, V-3). In all, three individuals across three generations (III-8, IV-2, V-1) were affected with DCM; of these, two (III-8, V-1) are still surviving. The proband's mother (IV-2) died from DCM at 27 years of age, which suggests that the transmission of this disease was in an autosomal dominant manner. Subject III-8 also presented with muscular dystrophy, along with one other relative (II-1) who died from this disease. Six other members of this family died of an unknown heart condition; of these, three individuals (I-1, III-4, III-10) are depicted in the pedigree. The proband (V-1) was diagnosed with DCM without conduction system defects. His CPK levels were found to be normal. At 13 years of age, the proband received a heart transplant after a three-week history of malaise. Tissue sections were obtained from his explanted heart. The histology of these samples demonstrated epicardial fibrosis that was typical of muscular dystrophy. Tissue from his mother's skeletal muscle also exhibited pathology that was suggestive of dystrophy (data not shown).

3.1.2.2 Mutation Analysis

An abnormal SSCP profile was observed for Patient 2 (III-2) during the analysis of LMNA exon 10 at both 10°C and 20°C (Fig. 6). DNA sequencing revealed heterozygosity for a single nucleotide transversion from C→A in codon 541, resulting in

Fig. 5. Partial Pedigree for Patient 2.

Squares indicate males; circles indicate females. Symbols with diagonal slashes represent deceased subjects. The proband is indicated by an arrow. Blue circles represent the individuals from which DNA samples were obtained. Individuals affected with DCM are shaded in black; those with an unknown heart condition are shaded in grey. Symbols with green squares correspond to individuals affected with muscular dystrophy. (+) and (-) indicates the presence or absence of the LMNA R541S mutation in the DNA samples of family members who were screened by SSCP/DHPLC/sequencing.

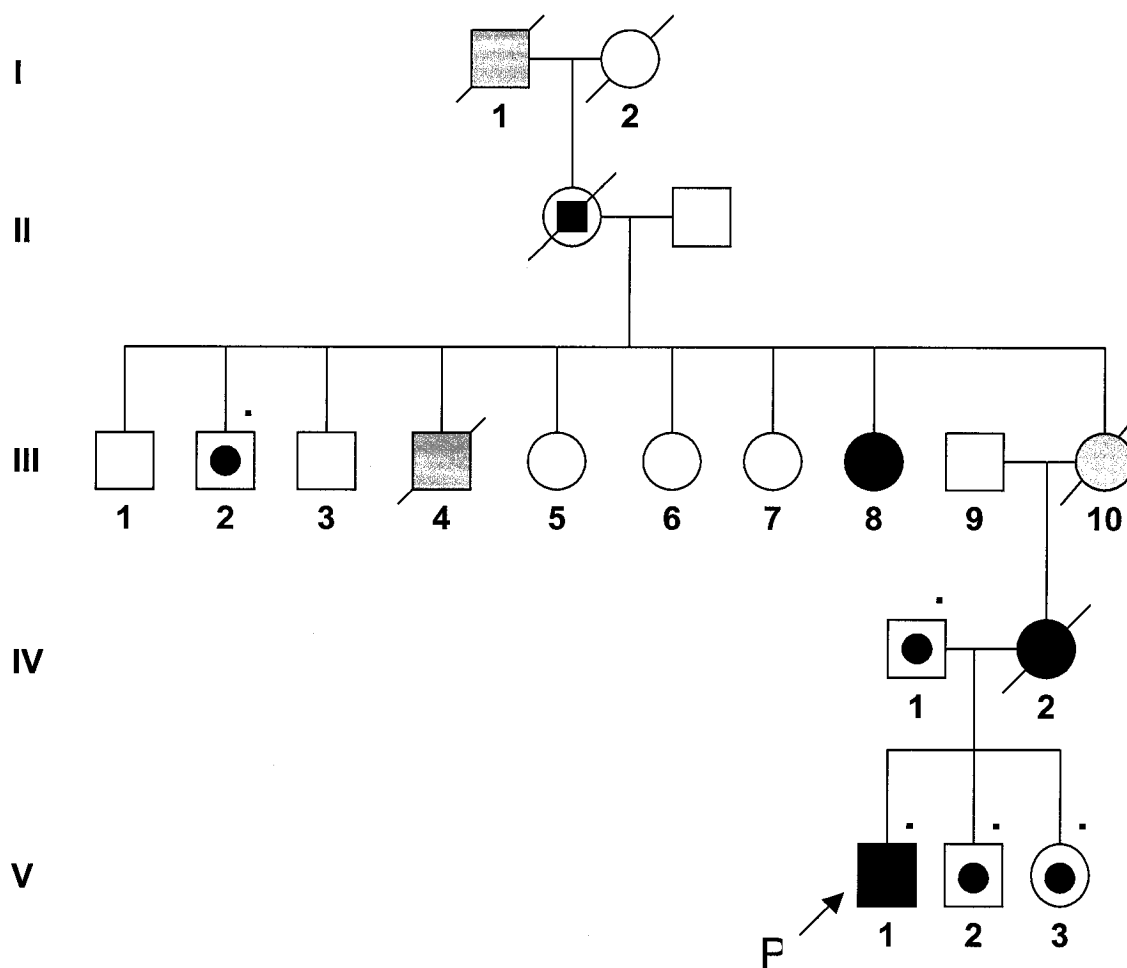
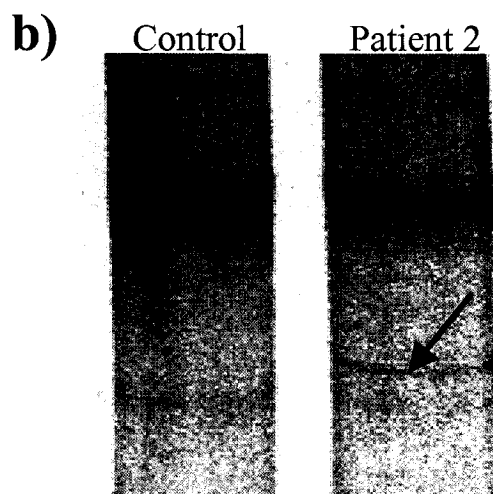
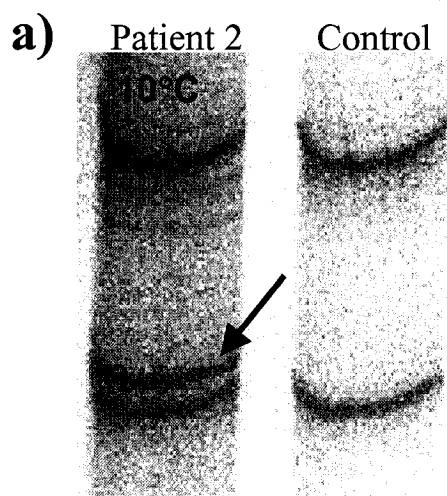


Fig. 6. SSCP Analysis of LMNA exon 10 from Patient 2 and a Control DNA Sample at 10°C and 20°C

Abnormal SSCP profiles obtained from Patient 2 during the screening of LMNA exon 10 at both a) 10°C and b) 20°C, as compared to control DNA samples. Red arrows indicate the mobility shift of ssDNA fragments due to a single base substitution.



a substitution of the wild-type arginine to serine (Fig. 7). This mutation was not observed in 200 control chromosomes (data not shown). However, both of the non-affected proband's siblings (V-2, V-3, aged 10 and 9 respectively) were found to be carriers of the R541S mutation (Fig. 5). The mutation is located in the intermediate filament tail, which forms part of the C-terminal globular head domain and is highly conserved among various species (Fig. 8).

3.2 Determination of the Expression of the Novel LMNA Mutations in Cardiac Tissue from DCM Patients

3.2.1 Electron Microscopy

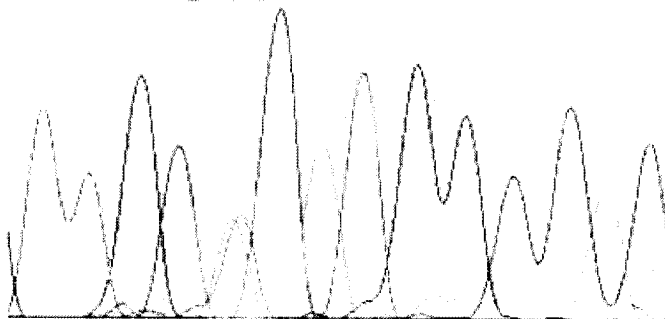
In order to assess whether these two novel LMNA mutations, D192G and R541S, would result in signs of nuclear membrane damage, tissue sections from the explanted hearts of DCM Patients 1 and 2 were examined under the electron microscope in collaboration with Dr. Veinot (Department of Pathology and Laboratory Medicine, University of Ottawa). Despite the fact that both patients presented with end-stage DCM at the time of their respective heart transplants, and both possessed LMNA mutations, there were huge discrepancies in the degree of pathological changes exhibited by the ultrastructural architecture of their cardiomyocytes (Fig. 9). Electron micrographs of the heart tissue sections from Patient 1 demonstrated dramatic morphologic alterations, including a complete loss of the nuclear membrane, the accumulation of mitochondria, glycogen and/or lipofuscin in the nucleoplasm, and chromatin disorganization in

Fig. 7. DNA Sequencing Electropherograms of LMNA exon 10 from Patient 2 and Control DNA

The reverse strand of LMNA exon 10 is depicted in this electropherogram. Highlighted area indicates the position of the G→T transition (i.e. the C→A transition in the forward strand), which leads to a substitution of the wild-type arginine (CGC) by serine (AGC) at codon 541 (R541S). Patient 2 is heterozygous for the R541S mutation.

Patient 2

130
T T G C H C A T G G C C A C
140
G → T



Control

140
T T G C G C A T G G C C A C
150

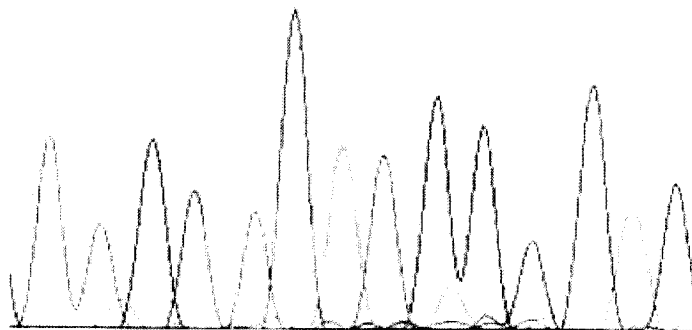
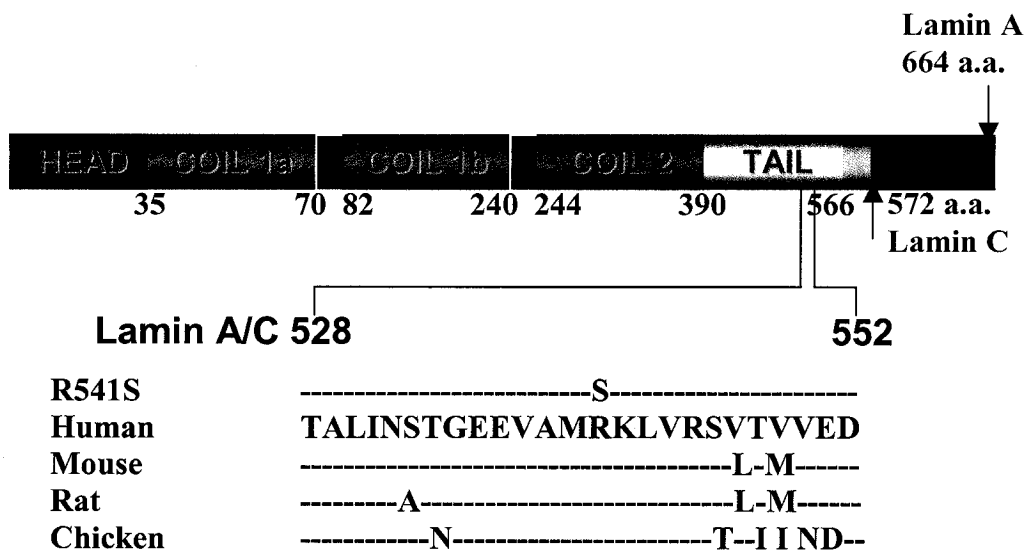


Fig. 8. Location of the R541S Mutation Within the Secondary Structure of Human LMNA

The mutation is located in the intermediate filament tail, which forms part of the carboxy-terminal globular head domain and is highly conserved among various species. The position of the affected amino acid is highlighted in yellow.



approximately 30% of nuclei (Fig. 9a, 9b). By contrast, examination of the heart tissue sections from Patient 2 revealed only modest and non-specific nuclear membrane alterations, comparable to those found in transplanted DCM patients without LMNA mutations (Fig. 9c, 9d).

3.2.2 Comparison of LMNA Expression in the Left Ventricle of End-Stage DCM Patients With or Without LMNA Mutations

In order to compare LMNA cDNA expression levels in explanted tissue samples from the left ventricle of end-stage DCM patients, quantitative RT-PCR was performed using the LightCycler and SYBR green technology. RNA from Patient 2, as well as two other end-stage DCM patients without LMNA mutations, was extracted from the flash-frozen heart tissue samples and reverse transcribed. The resulting cDNA was amplified for both LMNA exon 10 and GAPDH, a housekeeping gene, using real-time PCR with SYBR green dye as the means of detecting the amount of product obtained at the end of each amplification cycle. Prior to these experiments, standard curves consisting of six different dilutions, ranging from 100 pg/ μ l to 0.01 pg/ μ l were generated for both LMNA and GAPDH (Fig. 10). Subsequent cDNA yields were quantified relative to the 10 pg/ μ l dilution imported from these standard curves. The expression levels of the LMNA exon 10 cDNA were reported as the normalized ratio of LMNA-to-GAPDH. It is evident from these experiments that the heart tissue from Patient 2 was expressing LMNA cDNA at levels comparable to the two control samples (Fig. 11).

Fig. 9. Electron Micrographs of the Nuclear Membrane in LMNA Mutant and Wild-Type Cardiomyocytes

Tissue samples from the explanted hearts were fixed in 1.6 % gluteraldehyde, processed into thick and thin sections, and examined under a Hitachi 7100 electron microscope. Electron micrographs of the heart tissue sections from Patient 1 demonstrate a complete loss of the nuclear membrane (a) and the accumulation of mitochondria in the nuclear matrix (b). Patient 2 revealed only modest and non-specific nuclear membrane alterations (c), comparable to those found in transplanted DCM patients without LMNA mutations (d).

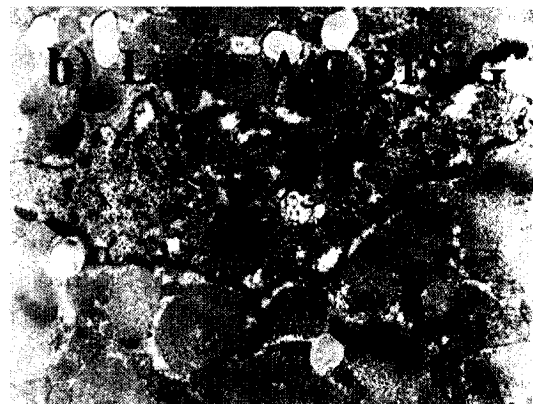


Fig. 10. Standard Dilution Curves for LightCycler Analysis of GAPDH and LMNA exon 10

Standard dilution curves were generated in duplicate for (a) GAPDH, a housekeeping gene, which was inserted into the pCR[®] 2.1-TOPO[®] vector according to the TOPO TA cloning kit, as well as (b) LMNA, which was inserted between the EcoR1 and BamH1 restriction sites on the pEYFP-C1 vector. The following dilutions were employed for both standard curves (shown from left to right): 100 pg/ μ l, 50 pg/ μ l, 10 pg/ μ l, 1 pg/ μ l, 0.1 pg/ μ l, 0.01 pg/ μ l.

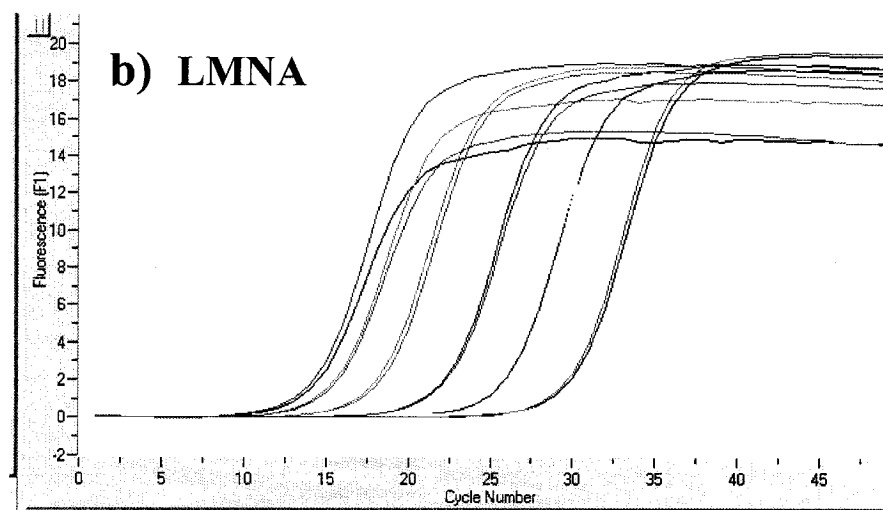
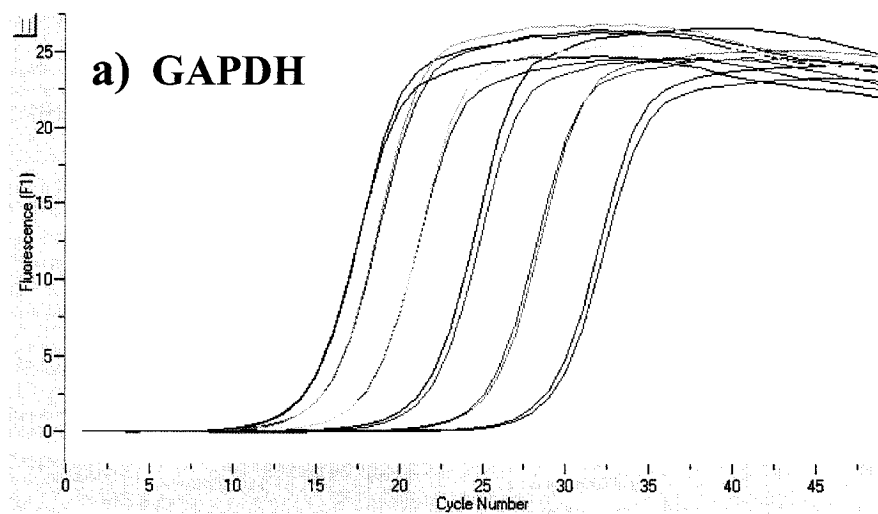
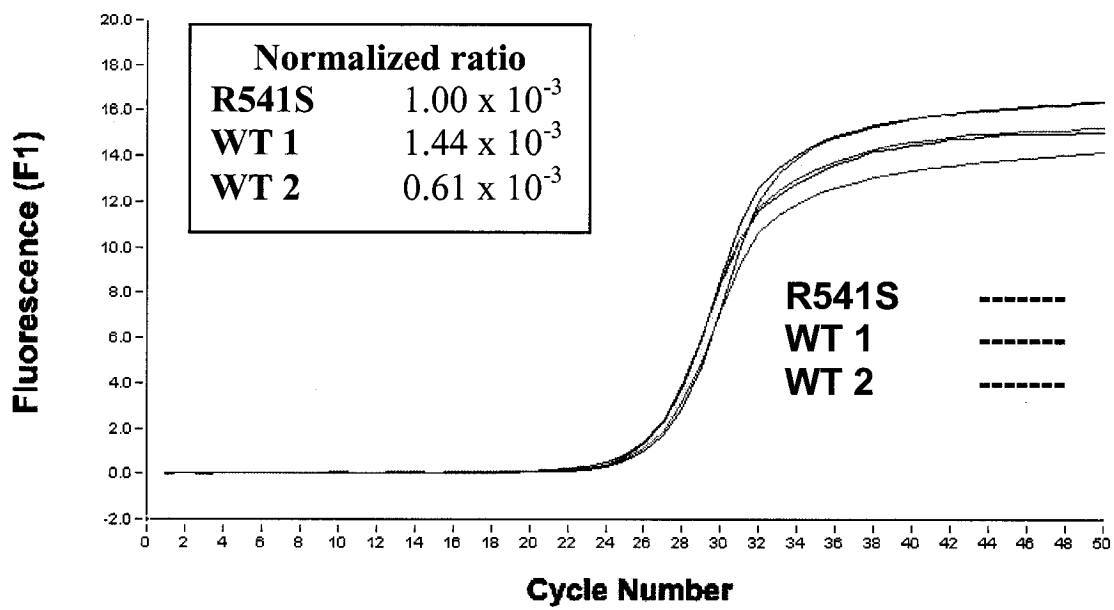


Fig. 11. SYBR Green RT-PCR Quantification of LMNA mRNA in the Heart Tissue Samples from Patient 2 and Two Wild-Type LMNA End-Stage DCM Patients

In this figure, both LMNA and GAPDH fragments were amplified from the cDNA of Patient 2 (R541S) as well as two other control subjects (WT 1, WT 2). The data was then analyzed in relation to the 10 pg/ul dilution from both the GAPDH (not shown) and LMNA standard curves. The expression of cDNA from Patient 2 is highlighted in red. Wild-type controls, WT 1 and WT 2 are shown in blue and green, respectively. Normalized LMNA-to-GAPDH ratios indicate that Patient 2 is expressing LMNA cDNA, and hence mRNA, at levels comparable to both controls.



3.2.3 Determination of the Relative Expression of the Wild-type vs the Mutated LMNA Allele in the Cardiac Tissue from Patient 2 and a LMNA Wild-type, End-Stage DCM Patient

In order to determine whether the relative absence of pathology in the cardiac myocytes of Patient 2 was due to the lack of expression of the LMNA R541S mRNA, a RFLP assay with HinP1 was performed on the cDNA obtained from the heart tissue of this individual. HinP1 was chosen because it had a restriction site at the precise location of the R541S mutation. The single nucleotide substitution from C→A would cause the restriction site to disappear, preventing the cleavage of the cDNA at this position. Therefore, the R541S cDNA would be cleaved by HinP1 into fragments of 97 bp and 17 bp in length, whereas the digestion of the wild-type LMNA cDNA would yield three fragments of 85 bp, 12 bp, and 17 bp in length (Fig. 12). In this assay, the LMNA exon 10 cDNA from the left ventricle and right atria of Patient 2, as well as an end-stage DCM patient with wild-type LMNA, were incubated with or without HinP1. As a result, a 97-bp fragment was produced in the case of the R541S mutation (Fig. 13). An 85-bp fragment was obtained by digesting wild-type LMNA exon 10 cDNA with HinP1. This band was also present in the cDNA of Patient 2, confirming the heterozygous nature of the R541S mutation. The 17 bp and 12 bp bands could not be visualized on the gel due to their diminutive dimensions. The same digestion performed on genomic DNA yielded a fragment of 506 bp. The results of this assay from the cDNA of the left ventricle were analogous to those obtained from that of the right atria. Therefore, it is possible to conclude with this experiment that the mutated LMNA exon 10 cDNA was expressed in the heart tissue of Patient 2.

Fig. 12. Cleavage of R541S and Wild-type LMNA cDNA by HinP1

HinP1 has a restriction site at the precise location of the R541S mutation, which is highlighted in red. The single nucleotide substitution from C→A would cause this restriction site to disappear, preventing the cleavage of the cDNA at this position. Consequently, the R541S cDNA would be cleaved by HinP1 into fragments of 97 bp and 17 bp in length, whereas the digestion of the wild-type LMNA cDNA would yield three fragments of 85 bp, 12 bp, and 17 bp in length.

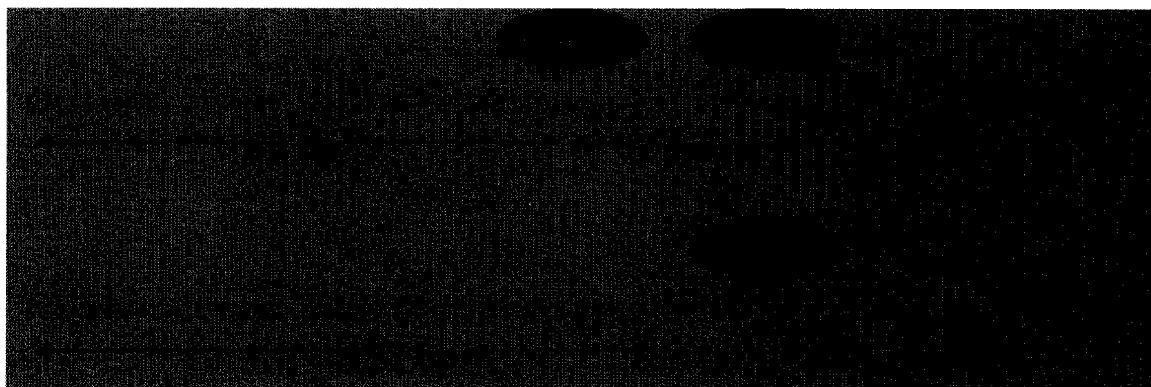
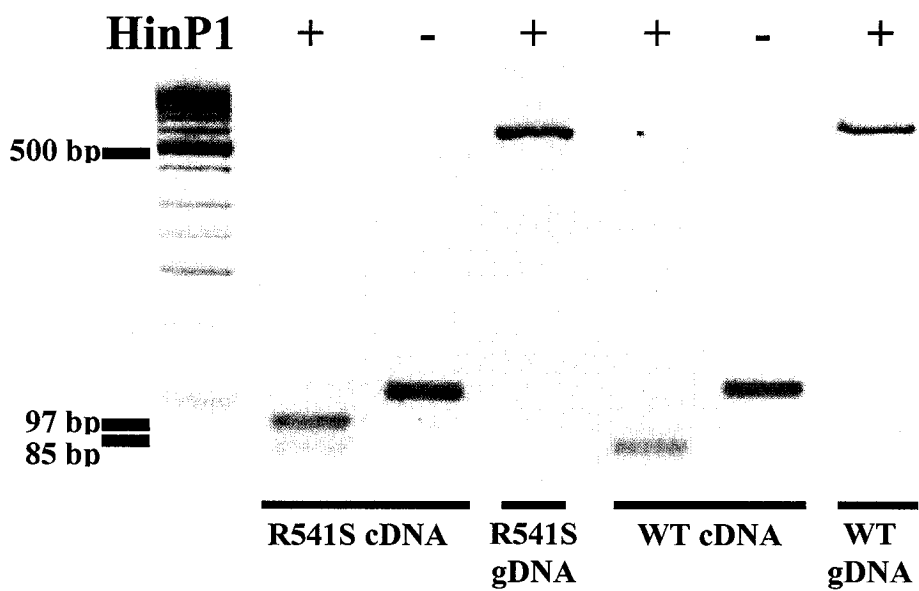
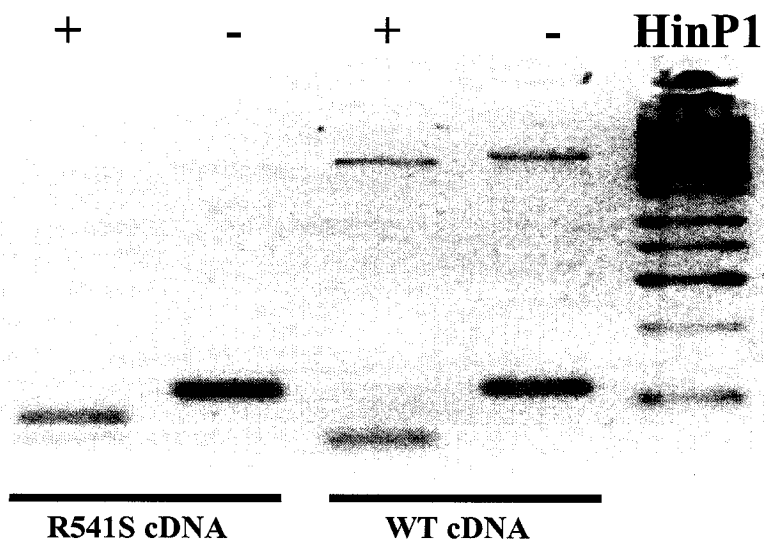


Fig. 13. R541S Allele Expression in Heart Tissue from Patient 2 Determined by HinP1 RFLP

LMNA exon 10 cDNA from the (a) left ventricle and (b) right atria of Patient 2, as well as one end-stage DCM patient with wild-type LMNA, was incubated in the presence or absence of HinP1.

- a) A 97-bp fragment was produced in the case of the R541S mutation (lane 1). An 85-bp fragment was obtained by digesting wild-type LMNA exon 10 cDNA with HinP1 (lane 4). This band was also present in the cDNA of Patient 2 (lane 1), confirming the heterozygous nature of the R541S mutation. The same digestion performed on genomic DNA yielded a fragment of 506 bp (lanes 3 and 6).
- b) The results of this assay from the cDNA of the right atria were analogous to those obtained from that of the left ventricle. Therefore, mutated LMNA exon 10 cDNA was expressed in the heart tissue of Patient 2.

a) Left Ventricle**b) Right Atria**

4 DISCUSSION

4.1 LMNA Mutations and Dilated Cardiomyopathy

In 1999, Fatkin et al. identified the first five LMNA mutations to be associated with autosomal dominant DCM in 11 families with conduction-system disease, but no signs of joint contractures or skeletal myopathy (76). Four of these missense mutations (R60G, L85R, N195K, E203G) were located in the alpha-helical rod domain of the LMNA gene, whereas the R571S substitution was found within the carboxy-terminal domain of lamin C (76). All of these mutations altered the charge of the encoded amino acid, and were thus predicted to influence the structure of the resulting protein.

The following year, Brodsky et al. identified the first nucleotide deletion in the LMNA gene (delT959) within exon 6 (111). The majority of the affected family members in this study possessed varying degrees of mild skeletal involvement (111). This LMNA deletion was predicted to produce an altered protein with a unique 158 amino acid addition to the carboxy-terminal end of the otherwise wild-type lamin A/C (111). Part of the rod domain involved in dimerization would remain intact, whereas the nuclear localization signal, lamin A processing site, and carboxy-terminus would be completely deleted (111). That same year, Genschel and Schmidt discovered another LMNA deletion (delA1397) in exon 8 and a missense mutation (R644C) in exon 11, which affected only lamin A (43). The patients in this study presented with a severe form of DCM, but without any skeletal muscle disease.

In 2001, Jakobs et al. reported two more LMNA mutations (E203K and R225X) that altered amino acids within the coil 1B domain (112). Recent evidence suggests that

the E203K residue is located within a stability-conferring region common to many intermediate filaments (112), whereas the R225X substitution leads to the production of a truncated protein containing approximately the initial third of lamin A/C (112). This mutant protein could act in a dominant negative manner by disrupting the alpha-helical rod structure of the lamins (112). Alternatively, nonsense-mediated decay could remove most of the transcribed mutant mRNA, causing disease via haploinsufficiency (112).

Two more studies in 2002 expanded the list of LMNA mutations and provided insight into the functional consequences of these genetic defects. Hershberger et al. identified a missense mutation (L215P) in exon 4 (11). An extremely high percentage (88%) of the affected individuals in this study population required pacemaker therapy, which suggests that even within the DCM disease subtype, certain lamin A/C mutations may confer phenotypic specificity (11). Arbustini et al. discovered five additional LMNA missense mutations (K97E, E111X, R190W, E317K, and a 4-bp insertion at 2869cDNA) in DCM patients with atrioventricular block (113). This study provides the first description of ultrastructural nuclear membrane damage associated with LMNA gene defects. Electron microscopy of the myocyte nuclear membranes revealed the presence of focal disruptions, bleb formation, and nuclear pore clustering (113). In addition, LMNA expression was notably reduced or absent in the myocyte nuclei (113). Western blot analyses of three hearts with different mutations demonstrated the presence of an additional 30 kDa band, suggesting a degrading effect of mutated LMNA on wild-type proteins (113).

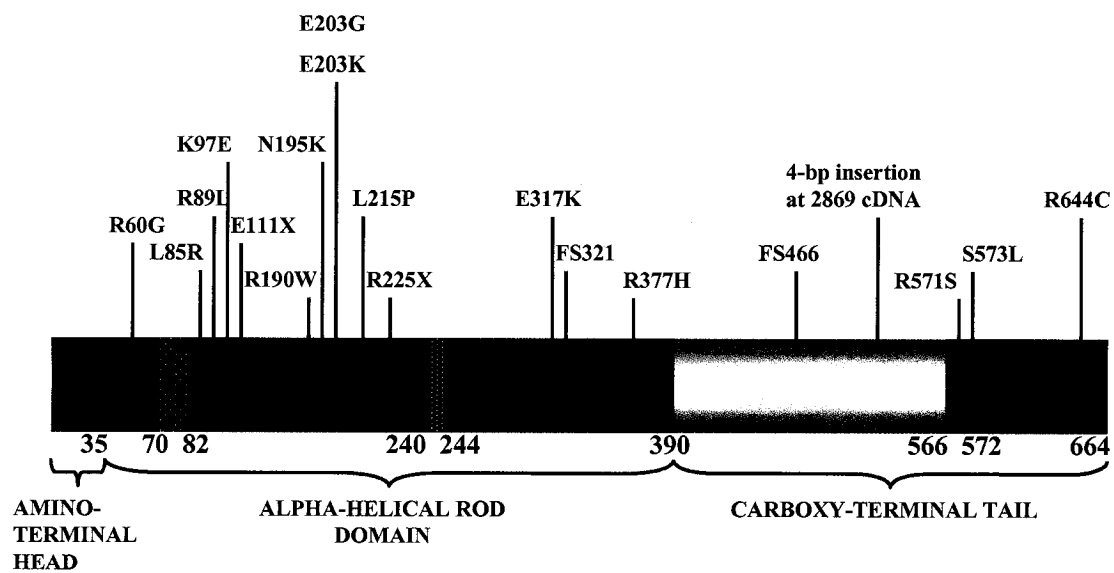
Earlier this year, Taylor et al. detected three additional LMNA missense mutations in DCM patients: R89L, R377H, and S573L (4). R89L is located in the highly

conserved alpha-helical rod domain and may disrupt the heptad pattern of coil 1b, which may adversely affect the dimerization and assembly of lamins A and C (4). S573L exchanges a hydrophilic residue for a hydrophobic one in the carboxy-tail of the lamin A isoform (4). This region controls the lateral assembly of protofilaments and mediates the lamin network formation (4). R377H occurs in a 30 amino acid segment at the carboxy-terminal end of the rod domain, which is conserved among lamins and cytoplasmic intermediate filaments and is critical for the higher order assembly of polymers (4). This same mutation has also been reported by Muchir et al. in an LGMD1B family (86). Indeed, Charniot et al. discovered yet another phenotype related to the R377H mutation (114). The clinical features of the family described in this report included cardiac involvement that preceded neuromuscular disease and a specific quadriceps myopathy (114). Cell transfection experiments demonstrate that the R377H mutation leads to mislocalization of both lamin and emerin (114). This new phenotype highlights the wide spectrum of neuromuscular and cardiac manifestations associated with lamin A/C mutations.

To date, mutations causing DCM have been reported in all the major regions of the LMNA gene, with the exception of the amino-terminal head domain (Fig. 14). Although important functions have been ascribed to lamin proteins, neither the location of these molecules nor their known functions provide conclusive insights into the mechanism by which conduction-system disease and DCM occurs in the cases of lamin mutations. These experiments will attempt to provide a foundation on which future studies surrounding the functional consequences and pathogenesis of LMNA mutations in DCM may be based.

Fig. 14. Localization of Published LMNA Mutations in DCM

This schematic outlines the linear representation of LMNA mutations in DCM, as well as the main regions of the LMNA gene. Mutations have been reported in the alpha-helical rod domain and the carboxy-terminal tail, but not in the amino-terminal head domain.
FS = frameshift.



4.2 The Identification of Novel LMNA Mutations in DCM

The main objectives of this part of the study were to: 1) expand on the existing list of LMNA mutations that would predispose individuals to DCM and 2) study the natural history of dilated cardiomyopathy. This was accomplished through the analysis of DNA extracted from blood samples via SSCP and/or DHPLC, followed by automated DNA sequencing in the event of an abnormal profile. Two novel LMNA missense mutations, D192G and R541S, were identified in two unrelated end-stage DCM patients from our study population. The location of these two mutations within the structure of the LMNA gene and protein may provide a basis from which the functional consequences of these genetic variations may be elucidated.

4.2.1 Lamin A/C Gene and Protein

The first part of exon 1 (amino acids 1-33) encodes for the amino-terminal head domain of LMNA (43;54;55). The region between the second part of exon 1 and exon 6 (amino acids 34-384) codes for the central alpha-helical rod domain, which consists of highly conserved heptad repeats (54). Exon 7 contains the nuclear localization signal (46;115). The remainder of the LMNA gene encodes the carboxy-terminal tail domains of lamins A and C (54). Alternative splicing within exon 10 generates two different mRNAs that code for lamin A and lamin C, which are only identical for the first 566 amino acids. Prelamin A contains 98 unique carboxy-terminal amino acids and is farnesylated at the CAAX box in this region after synthesis (43;70). Once prelamins A and C are incorporated into the lamina structure, they are converted into mature lamins A and C through endoproteolytic cleavage of the farnesyl group at Y646 of this CAAX box (52;70). In

contrast, lamin C has only 6 unique carboxy-terminal amino acids and does not require a prenylation procedure to be incorporated into the nuclear lamina (43;116;117).

All lamins share a common primary sequence consisting of globular amino- and carboxy-terminal domains separated by a central alpha-helical rod domain. This highly conserved rod domain is encoded by part of LMNA exon 1 to exon 6 (amino acids 34-384) and consists of four alpha-helical segments: coil 1a, coil 1b, coil 2a, and coil 2b (47;54). Hydrophobic heptad repeats within the highly conserved central rod domain promote formation of the alpha-helical coiled-coil dimer (43;46). Charged residues along the surface of this structure promote interactions between rod dimers, thereby producing complex assembly of the lamin filaments (53;118). Highly conserved residues found at both the amino- and carboxy-terminal ends of this protein play a crucial role in the association of lamin dimers into distinct higher order assemblies such as head-to-tail polymers (55). Further lateral interactions result in the formation of antiparallel protofilaments, up to eight of which associate to produce the characteristic 10 nm intermediate-like filaments (119). However, whether lamins assemble to form such structures in vivo within mammalian cells has yet to be satisfactorily resolved (119). The carboxy-terminal domains of both lamins have been shown to adopt a “type s” immunoglobulin-like fold (55). It consists of nine beta strands, forming two beta sheets of four and five strands each that are packed into a classical beta sandwich (55).

4.2.2 Location of Lamin A/C Mutations

D192G is located in the central alpha-helical rod domain at the distal end of coil 1b. Since this highly conserved region of the lamin A/C protein is critical for the formation of the alpha-helical coiled-coil dimer, the basic building blocks for the

construction of lamin filaments, a mutation in this area could easily be anticipated to have some disruptive effect on nuclear lamina assembly. This prediction appears to be supported by experiments in which lamin A/C proteins containing coil 1b mutations were expressed in HeLa cells (52). Although varying phenotypes were exhibited by these lamin mutants, all of them possessed an incapacity to assemble correctly into the nuclear lamina (52). However, it must be emphasized that these results were obtained from *in vitro* studies and may not necessarily reflect the true outcome of these mutations *in vivo*.

R541S is located within the region shared by both lamins A and C. The buried side chain of R541 participates in the stabilization of the carboxy-terminal beta-sandwich through hydrophobic contacts with the core of the domain (55). Such interactions may be disrupted with its mutation to serine. Structural determination of the carboxy-terminal domain strongly suggest that the mutations causing muscle-specific disease destabilize the lamin immunoglobulin-like domain, thus leading to a global loss of function of the A-type lamins (55). This is further supported by evidence that the nuclear lamina is associated with the inner nuclear membrane through interactions with integral membrane proteins via binding sites located in their carboxy-terminal globular tail (43;47;52). For example, previous studies indicate that the region spanning residues 319 to 572 binds the alpha-specific component of LAP2alpha (55). Furthermore, the area encompassed by residues 384 to 566 contains a binding site for emerin (55). A number of biochemical studies also suggest that the tail domain of lamins can bind directly to DNA, chromatin and core histones (55;63;65). More recent work has suggested that lamin A might make indirect interactions with the chromatin through a chain of interactions involving emerin and LAP2 (63;120). Finally, lamin A has also been shown to bind PKC-alpha at a site

downstream of residue 499 (77). PKC is a serine/threonine protein kinase known to occupy critical nodes in the complex signal transduction networks that regulate diverse cellular processes (77). Together, these findings suggest that a mutation of residue R541 could have disruptive effects on multiple functions of the A-type lamins, including the maintenance of nuclear architecture, the provision of anchorage sites for chromatin, and signal transduction.

4.3 Effect of LMNA Mutations on the Nuclear Architecture of Cardiac Myocytes from End-Stage DCM Patients

Electron microscopy was performed on tissue sections from the explanted hearts of DCM Patients 1 and 2 in order to assess whether these two novel LMNA mutations, D192G and R541S, would result in signs of nuclear membrane damage. Previously, Arbustini et al. completed a similar analysis on endomyocardial biopsies from DCM patients with the following LMNA mutations: K97E, E111X, R190W, and a 4-bp insertion at 2869cDNA (113). The ultrastructural study revealed the presence of “delamination”, focal ruptures, blebs and nuclear pore clustering of the myocyte nuclear membranes (113).

Similar morphological alterations of the nuclear membrane have been reported in carriers of LMNA mutations who are affected by other diseases. Electron micrographs of muscle biopsies from autosomal dominant EDMD patients with LMNA mutations reveal the presence of misplaced heterochromatin and nuclear pore aggregates within the affected nuclei (121). In addition, the nuclear membrane of these nuclei was not clearly visible (121). A subpopulation of skin fibroblasts from Dunnigan-type familial partial

lipodystrophy patients harboring LMNA R482Q or R482W mutations also contained nuclei that demonstrated abnormal blebbing, with a frequently disorganized peripheral meshwork of A-type lamins (122). Cells from lipodystrophic patients often had other defects, mainly consisting of nuclear envelope herniations that were deficient in B-type lamins, nuclear pore complexes, LAP2beta, and chromatin (122). Fibroblast nuclei from individuals affected with mandibuloacral dysplasia also exhibited similar abnormalities (102). At least 10% of the nuclei from carriers of the R527H mutation possessed a “honeycomb” distribution of lamin A/C (102). In addition, a small percentage of the homozygous fibroblasts were characterized by the presence of lobulated nuclear envelopes (102).

These changes in nuclear morphology are mirrored in various animal models with LMNA mutations, ranging from mice to flies. For example, 58% of the embryonic fibroblasts from the L530P homozygous mice created by Mounkes et al. displayed disruptions of the nuclear membrane (45). These herniations consisted of discrete locations in which the inner and outer nuclear membranes appeared to lose contact with each other, resulting in the expansion of the perinuclear space and ballooning of chromatin into a bleb-like structure. This large-scale herniation was also observed in over 80% of the embryonic fibroblasts obtained from LMNA null mice, which lack the region of the LMNA gene extending from exon 8 to the middle of exon 11 (62). A slight degree of nuclear pore clustering was also revealed in some LMNA^{-/-} nuclear envelopes (62). Ultrastructural examination of the LMNA^{-/-} mouse embryonic fibroblasts and hepatocytes demonstrated a thinning or loss of heterochromatin at specific sites on the inner nuclear membrane (62). These segments of the nuclear envelope, which also lack

morphologically identifiable nuclear pore complexes, likely correspond to areas of nuclear herniation. All of these observations complement those from a previous study of *Drosophila* mutants, in which reduced lamin Dm₀ expression led to the development of defective nuclear envelopes (123).

Based on these findings, it was postulated that the cardiac myocytes from the two carriers of LMNA mutations in this study would also demonstrate indications of nuclear membrane damage. Both presented with end-stage DCM at the time of their respective heart transplants and both possessed LMNA mutations, albeit in different domains of the lamin A/C protein. Therefore, the fact that there were major discrepancies in the degree of pathological changes exhibited by the ultrastructural architecture of their cardiomyocytes came as a complete surprise. Heart tissue sections from Patient 1 (D192G heterozygote) revealed a total loss of the nuclear membrane and the accumulation of mitochondria in the nuclear matrix (Fig. 9a, 9b). By contrast, cardiac myocytes from Patient 2 (R541S heterozygote) presented only modest and non-specific nuclear membrane alterations, comparable to those found in transplanted DCM patients without LMNA mutations (Fig. 9c, 9d). It is clear from these observations that direct correlations between any of the morphological changes and the mutations cannot be made.

A number of factors may have contributed to the discrepancies in nuclear morphology exhibited by these two end-stage DCM patients. First of all, since the D192G and R541S LMNA mutations are located in different domains, they may affect the nuclear lamina organization and the function of the lamin A/C protein in a different manner. Indeed, the various functions and interactions of the rod and carboxy-terminal

domains are unique. The effects of muscle damage and the varying ages of the patients also needs to be considered, especially since penetrance is shown to increase with age. It is remotely possible that the pathology exhibited by the cardiomyocytes of Patient 1 was more severe simply because he was fourteen years older than Patient 2 at the time of tissue collection.

4.4 Expression of the Wild-Type vs. the Mutated Allele in the Cardiac Tissue of End-Stage DCM Patients With or Without LMNA Mutations

One plausible explanation for the relative absence of pathology exhibited by the cardiac myocytes of Patient 2 is that the R541S mutation could have introduced an element of instability into the mutant LMNA mRNA, which could subsequently lead to a decreased, or total lack of, expression of the mutated allele. Northern blots performed on cell lines obtained from L530P homozygous mice detected a decreased level of LMNA transcripts, suggesting that the mutant mRNA was unstable (45). These results were confirmed by Western blots, which revealed that the quantity of mutant lamins A and C were concurrently diminished (103). Decreased levels of A-type lamins were also observed in the myocardial tissue of an EDMD patient with a LMNA nonsense mutation, E6X (124).

Therefore, in order to compare the expression levels of LMNA mRNA within the affected left ventricles of our end-stage DCM patients, quantitative RT-PCR was performed using the LightCycler and SYBR green technology. This method offers a more sensitive approach for the detection of slight differences in the quantity of mRNA than the standard Northern blot. The normalized ratios of LMNA-to-GAPDH obtained

from two trials of this experiment conclusively revealed that the left ventricle of Patient 2 was expressing LMNA exon 10 cDNA at levels comparable to the control samples, which were obtained from end-stage DCM patients without LMNA mutations (Fig. 11). This suggests that the introduction of the R541S mutation did not result in the instability of the LMNA mRNA.

A RFLP assay with *HinP1* was subsequently performed on the cDNA obtained from the heart tissue of Patient 2 in order to determine whether the relative absence of pathology in the cardiac myocytes was due to the lack of expression of the LMNA R541S mRNA. *HinP1* was chosen because it had a restriction site at the precise location of the R541S mutation. Cleavage of the mutated cDNA with this enzyme would yield a characteristic 97-bp band (Fig. 13). The fact that this band was clearly visible in samples from both the left ventricle and the right atria of Patient 2 provided indisputable evidence that the mutated LMNA exon 10 cDNA was indeed present in the heart tissue of this patient. Moreover, automated DNA sequencing of the cDNA obtained from Patient 2 confirmed the presence of the heterozygous R541S mutation (data not shown). This strongly suggests that the extreme differences in the degree of nuclear membrane disruptions exhibited by these two DCM patients cannot be explained by a lack of expression of the R541S allele.

4.5 Model Mechanisms for Autosomal Dominance of LMNA Mutations

The question as to the mechanism of autosomal dominance in the case of LMNA mutations and DCM remains unsatisfactorily answered to date. Several theories abound concerning the manner in which these mutations contribute to the disease phenotype.

One is haploinsufficiency, in which the reduced level of functional lamin A/C is insufficient for normal lamina production (80). In other words, a low level of expression or the rapid degradation of the mutant lamin protein may lead to the pathology that is associated with DCM. This hypothesis is supported by the fact that the nonsense mutation (E6X) discovered by Bonne et al. in an autosomal dominant EDMD family, produces a truncated protein of only five amino acids, which suggests that it is non-functional (53). However, pulse-chase experiments performed by Ostlund et al. showed no decrease in the stability of several mutant lamins (125). In addition, the heterozygote LMNA^{+/-} mouse contains only 50% of wild-type LMNA levels, but displays neither an EDMD phenotype nor a significant nuclear abnormality (62). Therefore, a simple haploinsufficiency of A-type lamins cannot be the only mechanism underlying the pathology of DCM.

It has been suggested that the majority of LMNA mutations may actually perpetuate a dominant negative effect that modifies, either directly or indirectly, the lamina and nuclear envelope (53;82;126). This mechanism is particularly consistent with LMNA mutations that impair dimerization (126). For example, the missense mutations discovered by Fatkin et al., located within the central rod domain of lamins A and C, are postulated to act as dominant negative alleles (76;83). Using the same reasoning, the D192G mutation found in Patient 1 of our study would also be expected to have a dominant negative effect on the assembly of the nuclear lamina, which may explain the complete loss of the nuclear membrane that was observed on the electron micrographs. Substitution of conserved residues in this central alpha-helical domain could potentially affect lateral interactions between lamin A/C rod dimers and prevent multimeric filament

formation. However, dominant negative effects are not limited to LMNA mutations found solely within this highly conserved rod domain. Mutations in exon 11 (G608G and G608S), which result in an incompletely processed prelamin A, are also predicted to act in a dominant negative fashion, because lamin A is known to form a multiprotein complex within the nuclear membrane (103).

In addition, LMNA mutations may hinder the contribution of normal lamin A/C proteins to the generation of higher level protein structures (4;83). Support for this hypothesis comes from recent studies in which lamin A mutants were overexpressed in cultured muscle cells (80;125). It was demonstrated that some of the transfected mutants could partially disrupt the endogenous lamina by altering the distribution of wild-type lamins (52;70;125). These alterations in nuclear morphology may be due to the relocation and/or degradation of wild-type lamins. It has been shown that mutated lamin C will precipitate the removal of wild-type lamin A to the nucleoplasm (52). The absence of LMNA immunostaining and the presence of low molecular weight (~30 kDa) fragments in the heart tissue of patients with K97E or E111X mutations provides some evidence that abnormal A-type lamins may induce degradation of the normal allele product (113). If this is indeed the case, terminally differentiated cells, such as cardiac myocytes, will be progressively depleted of A-type lamins. Furthermore, the low LMNA mRNA levels present in those cells will not be able to sustain a proportional increase in translation of LMNA mRNA to compensate for the increased degradation rate. However, it is very unlikely that a dominant negative effect was exerted by the R541S mutation identified in our study, as the nuclear membrane of the cardiac myocytes from Patient 2 remained relatively intact. In addition, the existence of three early termination mutations

causing autosomal dominant EDMD, one of which would terminate protein synthesis after only six amino acids, presents a major problem for this hypothesis (53;80). Unless alternative splicing or alternative initiation can produce a defective lamin from this allele, it would seem that a 50% reduction in LMNA levels is equally pathogenic (80).

Another possibility is that LMNA mutations may have dominant effects on the composition and function of the peripheral endoplasmic reticulum. The inner nuclear membrane (INM), outer nuclear membrane (ONM), and endoplasmic reticulum (ER) form a single continuous system containing functionally distinct domains, into which specific membrane proteins are segregated (119). Loss of lamin A/C causes the mislocalization of emerin from the INM to the ER (119;125). The implication is that the nuclear lamina plays an essential role in organization of this domain by maintaining the segregation of some INM proteins from the ONM and peripheral ER. Thus, the tissue specificity that is associated with diseases caused by LMNA mutations may be ascribed to the impaired function of particularly sensitive processes enacted by the ER (119). For example, the ER is the major site of cholesterol regulation and fatty acid synthesis. Abnormal accumulation of proteins in the ER could alter lipogenesis or lipogenic signaling in LMNA-deficient cells, resulting in aberrant adipocyte development and lipodystrophic disease (119). In the case of skeletal and cardiac muscle, Ca^{2+} release during contraction cycles may be compromised by alterations in the sarcoplasmic reticulum, which is also contiguous with the ER in muscle tissue (119). Alternatively, generalized stress due to inappropriate accumulation of nuclear envelope proteins, such as emerin, in the ER could promote aberrant intracellular signaling pathways with downstream effects on gene expression and cell viability (119).

Therefore, the only clear conclusion that we can draw from these hypotheses is that there is no definite answer to the mystery of the mechanism underlying the autosomal dominance of LMNA mutations in DCM. For every experiment that seems to support one of these models, there are others that directly refute its claims. Further research is needed to shed more light on this matter.

4.6 Pathogenic Mechanisms of LMNA Mutations

With every novel finding that each study brings to the growth of knowledge surrounding the effects of LMNA mutations, more questions are brought to the forefront. However, answers to some of the fundamental issues underlying this field of research remain based on mere conjecture. Two of the most basic questions concerning the consequences of LMNA mutations are still under debate. First of all, why do ubiquitously expressed nuclear envelope proteins give rise to tissue-specific disease phenotypes? Secondly, what exactly accounts for the huge range of phenotypic heterogeneity that is observed in carriers of LMNA mutations? Several of the most popular hypotheses are delineated below.

4.6.1 Mechanical Stress Model

In the “mechanical stress” hypothesis, mutations in lamins A and C are thought to weaken the structural integrity of an integrated nucleocytoplasmic skeletal network (70). This model is often invoked to provide explanations for the pathogenesis of EDMD, LGMD, and DCM. Since skeletal and cardiac muscle cells do not express lamin B1, they might be unusually dependent on A-type lamins, as well as their binding partners, to withstand contraction forces (47;49;84). Alternatively, muscle cells might depend on

lamins A/C for other functions, such as anchoring emerin within the nucleus. If the absence of emerin or the presence of LMNA mutations manages to destabilize the association of lamins with the nuclear envelope, the lamina as a whole would become less effective as a load-bearing structure (47;84). Therefore, mechanical stress, and possibly the flattening of nuclei at the periphery of the muscle fiber or mature adipocytes, could enhance the fragility of the integrated network already induced by LMNA mutations or a lack of emerin (70). This general fragility would eventually translate into cell death and tissue damage. For example, lamina in fibroblasts from human subjects with Dunnigan-type familial partial lipodystrophy have been shown to possess a low resistance to stress induced by heat shock (70). In skeletal muscle, the damage might be limited because muscle fibres are a syncytium, and not all of the nuclei may be affected within a single fibre. On the other hand, loss of individual cardiomyocytes in cardiac muscle would be cumulative and would eventually lead to conduction blocks (47;69). Therefore, the etiology of these muscle-related diseases can be explained by an accumulation of damaged nuclei, resulting from a reduction in the load-bearing properties of the lamina (47).

4.6.2 Gene Expression Model

Although the mechanical stress model may provide a sufficient explanation for the pathogenesis of muscle-related diseases, it does not account for the other disorders associated with LMNA mutations. For example, it is nearly impossible to reconcile the puberty-associated loss of adipose tissue found in Dunnigan-type familial lipodystrophy with this hypothesis because adipocytes are not contractile (49). An alternative model is that LMNA-associated pathology may be caused by subtle defects in gene expression

(49). Since lamin complexes are involved in tissue-specific gene regulation, mutations in any of its components may ultimately promote the pathophysiology of various diseases (84). Numerous studies have provided evidence that the nuclear lamina is intimately associated with mediators of genetic expression. For example, lamins are known to interact with various transcriptional regulators, such as retinoblastoma protein (p110Rb) and BAF1 (47;55;127). Lamins also bind transcription factors, such as sterol regulatory element binding protein-1 (SREBP-1); it is possible that a disruption of this interaction in adipocytes may explain why lipodystrophy occurs in humans with mutated LMNA and in mice transgenic for SREBP-1 (126). One of the INM proteins shown to interact directly with the nuclear lamina, the lamin B receptor, could also influence gene expression through its binding to HP1 protein (80). In *Drosophila*, HP1 suppresses the expression of normally active euchromatic genes translocated near heterochromatin (125;128). Moreover, dynamic studies demonstrate that peripheral chromatin is associated with the highly stable interphase nuclear lamina (70). Hence, alterations in lamina structure induced by LMNA mutations could relax these constraints and instigate a tissue-specific change in the pattern of gene expression (70). It should come as no surprise, then, that alteration of the nuclear lamin organization would inhibit RNA pol II-dependent transcription (75). Loss of specific attachment sites on the nuclear lamina could therefore lead to defects in tissue-specific gene expression and amplify the consequences of LMNA mutations (55).

Unique combinations of lamins and lamin-associated proteins are present in various tissues during development and cell differentiation (69). It is a known fact that changes in lamin expression often correlate with transitions in these two cellular

processes (49). For example, the expression levels of A-type lamins increase with terminal differentiation and growth arrest (55). Previous studies in animal models indicate that lamins A and C are absent from all preimplantation stage embryonic cells (including embryonal carcinoma cells), with their synthesis commencing at about day 9 within the visceral endoderm and trophoblast (62;129). Henceforth, A-type lamins appear asynchronously in various tissues; certain cell types may not even express these proteins until after birth (130). In summary, lamins can bind numerous transcriptional regulators, and are differentially expressed along with other nuclear envelope proteins. This suggests a model in which distinct combinations of these factors could create unique platforms for a variety of proteins involved in signaling, DNA replication, and the modification or organization of chromatin structure (49). Indeed, ectopic expression of lamin A in myoblasts has been reported to induce the synthesis of muscle-specific genes (47). Thus, it has long been thought that lamins may possess some influence on the capacity for gene expression, although the exact mechanism by which this is accomplished remains to be elucidated (49).

4.6.3 Putative Models of Pathogenesis for the D192G and R541S LMNA Mutations Expressed in End-Stage DCM Patients

D192G is located in a highly conserved region of the lamin A/C protein that is critical for the formation of the alpha-helical coiled-coil dimer, which is the basic building block of nuclear lamina filaments. A mutation at this location could therefore conceivably disrupt the construction of the highly organized structure of the peripheral nuclear lamina network. For example, dimer formation, head-to-tail assembly of dimers, or lateral assembly of complex filaments could be adversely affected. This, in

part, could explain the complete absence of the nuclear membrane that was observed from the electron micrographs of the cardiac myocytes obtained from Patient 1.

However, the pathology exhibited by Patient 1 may only represent an extreme case of the functional consequences of a missense mutation located in this highly conserved central alpha-helical rod domain. Instead of a complete loss of function, the nuclear membrane may only sustain mild degenerative changes in certain areas but remain relatively intact in others, depending on the ability of the mutated lamin protein to assume the appropriate coiled-coil dimer formation. These lamin-deficient areas would then be more susceptible to mechanical stresses generated by contraction of the cardiac myocytes.

Although the R541S mutation is not located within the LMNA domain that is required for dimer formation, it is found within a region of the carboxy-terminal globular tail that has been shown to interact with a variety of different proteins. For example, A-type lamins are essential for the retention of emerin at the nuclear periphery (52). Mislocalization of this integral protein could represent an alternative route by which the structural integrity of the nuclear membrane is compromised. Hence, the mechanical stress model could also be used to provide an adequate explanation for the pathogenesis of the R541S mutation. However, the structural pathology exhibited by cardiomyocytes possessing R541S lamin A/C may be less drastic than that observed in the heart tissue of Patient 1, simply because this mutation does not affect the formation of the basic building blocks required for lamina assembly. Thus, only modest and non-specific structural changes may be noted, as demonstrated in the electron micrographs obtained from Patient 2. This does not preclude the possibility that interactions with other proteins, such as LAP2alpha, histones, transcription factors, and PKC may not have been adversely

affected by the R541S mutation. Although the nuclear structure of the cardiac myocytes from Patient 2 appeared to be relatively intact, the functional consequences of the R541S mutation could have been manifested as alterations in gene transcription and expression, which would not have been detected through electron microscopy.

4.7 Phenotypic Diversity of LMNA Mutations and the Role of Modifier Genes

One of the main difficulties in determining the pathogenic mechanism underlying the diseases associated with LMNA mutations is the fact that there is an abundance of clinical and phenotypic heterogeneity. Initial reports suggested that DCM associated with conduction defects resulted from mutations in the rod domains of lamins A and C. However, more recent data have indicated that there is no clear correlation between clinical phenotype and the location of LMNA mutations (70). In other words, there is no disease-restricted domain in LMNA (54).

To complicate matters even further, the same LMNA mutation could lead to multiple phenotypes in unrelated families (114). For example, an R527P mutation was associated with both lipodystrophy and EDMD in one patient (131), but only classical EDMD in other families (53;54;82). Brodsky et al. also demonstrated that a single mutation could result in multiple phenotypes, such as DCM in conjunction with conduction defects or various extracardiac findings, consisting of either EDMD or LGMD-like symptoms (111). In addition, phenotypic heterogeneity has been documented among affected members of the same family with the same mutation (114). For example, a specific LMNA mutation could elicit the full syndrome of EDMD on one side of the family, but the affected individuals in another branch may only exhibit cardiac

abnormalities (81). Even both of the patients within our study were found to have slightly varying DCM phenotypes. Patient 1 presented with a one year history of progressive heart failure with mild conduction system disease, whereas Patient 2 had no conduction defects. Although both subjects possessed normal CPK levels, histology of explanted heart tissue samples from Patient 2 demonstrated epicardial fibrosis typical of muscular dystrophy. In contrast, Patient 1 had no indications of muscle disease. Moreover, a mutation within the same pedigree may vary in its degree of penetrance and may exert either dominant or recessive effects (82). These findings highlight the difficulties that are inherent in diagnosing patients with DCM based solely on phenotypic differences.

Given the high degree of interfamilial and intrafamilial variability found among carriers of LMNA mutations, it was suggested that disorders affecting striated muscles (i.e. EDMD, LGMD, and DCM) could probably be considered as a single disease with a spectrum of clinical manifestations (70). It was also proposed that Dunnigan-type familial partial lipodystrophy (FPLD) and MAD could be classified separately as lipodystrophy syndromes, because both disorders are characterized by regional adipocyte loss and insulin resistance. CMTB1, which primarily affects nerve cells, was thought to constitute a third distinct group (70). At the time, there did not appear to be any overlap between these three categories. However, Garg et al. recently described two families diagnosed with Dunnigan-type FPLD who have cardiac conduction system defects and other manifestations of cardiomyopathy (70;132). In addition, there were reports of CMT families presenting with cardiomyopathy and adipose tissue abnormalities (99;133). Furthermore, the discovery that both mandibuloacral dysplasia and Hutchison-Gilford

progeria syndrome are associated with LMNA mutations provided an additional complication for the implementation of this generalized scheme. As the amount of research surrounding this subject accumulates over time, it becomes more and more evident that these disorders cannot be separated into distinct categories.

Ultimately, the variable degree of affected skeletal and/or cardiac muscle may depend on the form of the mutation, its site and co-precipitating factors (43). The extensive range of phenotypic heterogeneity points towards a possible role for modifier genes or other environmental factors (54). A potential susceptibility factor involves the possession of an abnormal immune response (10). High frequencies of cardiac autoantibodies in isolated DCM have been identified, which suggests that an immune response, independent from human leukocyte DR4 antigen, is activated (10). Although there is no conclusive evidence that these antibodies are directly pathogenetic, they may represent reliable markers of autoimmunity and may predict early disease among relatives at risk of developing DCM (10). Other susceptibility genes associated with the disease include those which encode the following proteins: PAF acetyl hydrolase, which acts as a defence against oxidative stress (134); manganese superoxide dismutase, an anti-oxidant enzyme (135); nebulin, an actin-binding Z-disc protein (136); and aldosterone synthase, which participates in the synthesis of mineralocorticoids (137). The influence of environmental factors on genetic expression is also illustrated by the fact that the phenotype of Dunnigan-type FPLD is often more prominent in females than in males (43;97). This suggests that changes in the hormonal or metabolic milieu trigger the expression of the specific histological and anatomical changes in carriers of these specific LMNA mutations (89).

Phenotypic diversity may also result from epigenetic inheritance, which has received little attention in clinical medicine (5). Alternatively, the solution may entail an even more simple and obvious explanation. Like other intermediate filament proteins, lamins form dimers by polymerizing in a head-to-tail fashion, although it is currently unclear whether these are homodimers or heterodimers in vivo (5). In either case, since both lamin A and C are encoded by the same gene, mutations within the common head or rod domains could potentially result in phenotypic diversity. A variety of dimer types (ex. AA, AA*, CC and CC*, where the asterisk indicates a mutation) may form, even in patients who are homozygous for a single mutation in the LMNA gene (5). Such a mutation would represent an unusual mechanism for phenotypic diversity, which is generally ascribed to the effects of modifying genes.

4.8 Study Limitations

The results of these experiments must be interpreted according to the limitations that are inherently imposed by this type of research. DCM has proven to be quite difficult to dissect genetically. Several reasons could explain this phenomenon. The penetrance of this disease is generally incomplete and age-related, which complicates the diagnosis (7;37). In addition, families are rarely genetically informative due to the severity of the disease (7;37). The five-year mortality rate is 50% after symptoms develop (3). Consequently, multigeneration DCM families with many affected, living individuals have been extremely difficult to identify and recruit. Perhaps the largest drawback is the fact that the technique of positional cloning, which enables the primary cause of disease to be defined without making a priori assumptions, cannot be used in

most DCM studies due to the inadequate participation or availability of family members. Although chromosomal loci for idiopathic DCM have been identified by genetic linkage analysis in rare families, even these families are considered to be insufficient for positional cloning (14).

Consequently, most researchers have turned to the candidate gene strategy in order to discover potential morbid genes among large cohorts of DCM patients (37). However, this approach is heavily dependent on prior assumptions and may thus be prone to false positives (138). For example, the initial association of alpha-actin mutations with pure DCM may have initiated a bias towards screening for mutations in sarcomeric or cytoskeletal genes. It is extremely possible that other relevant disease-causing genes may have been overlooked in this random selection process. Unfortunately, the very situations in which such a strategy is used (i.e. small families with insufficient power for linkage), are those in which candidate gene analyses are most susceptible to error (138). Another difficulty with this approach lies in differentiating between disease-causing mutations and neutral polymorphisms (37;138).

Therefore, safeguards have been built into these experiments to ensure the validity of a mutation discovered via this approach. One of these methods is to verify that the variant is present only in affected subjects. It should also be absent from a large population of ethnically-matched controls. In our study, both the D192G and R541S substitutions were not found in 200 control chromosomes obtained from a random sample of healthy individuals or other non-affected members of the family. In addition, the demonstration that the affected residue is highly conserved among different species lends support to the possibility that the substitution is indeed a disease-causing mutation, and

not just a polymorphism. Ultimately, reproducible identification of mutations in well-characterized populations and compelling functional data will be required to strengthen the case for specific mutations (138). The analysis of mutated LMNA mRNA expression levels in the cardiac tissue of end-stage DCM patients provides a basis on which to base future functional studies. At present, however, information for patients should not rely on molecular genetics, but rather on clinical examination, identification of pre-clinical signs and of asymptomatic patients, prevention of life-threatening ventricular arrhythmias, and counselling (139).

4.9 Clinical Implications

An immediate clinical benefit from the discovery of human gene mutations is early and accurate diagnosis (1). Improved recognition and intervention in advance of heart failure has considerable merit for reducing the serious morbidity and mortality associated with the disorders (1). The vast range of overlapping phenotypes and severity of symptoms associated with the varying “laminopathies” emphasizes the importance of regularly screening LMNA gene carriers who have no current evidence of disease (11). Periodic echocardiographic and electrocardiographic testing should be performed in an effort to identify and treat disease during its earliest stages. Adult LMNA mutation carriers should be screened annually, while those of unknown genetic status, who are also considered to be at risk, should be checked every three to five years (11). The availability of DHPLC with targeted sequence analysis makes mutation screening efficient and feasible. Prospective analysis of patients with skeletal and/or cardiac myopathy should include the characterization of glucose, insulin, and lipids, due to the

overlapping phenotypes of LMNA mutations (140). This should also be performed as a safeguard in order to compensate for the difficulties inherent in diagnosing patients based on phenotypic manifestations.

It is obvious from the mass of conflicting findings and postulated mechanisms of pathogenesis that have accumulated surrounding the role of LMNA mutations in DCM, that this disease is extremely difficult to dissect genetically. The only concrete conclusion that can be drawn at this point was once succinctly stated by H.L. Mencken: “for every complex problem, there is an answer that is clear, simple, and wrong”. However, each “wrong” answer is one step closer to the “right” ones. Although the whole picture is not yet in sight, individual pieces are falling in place one experiment at a time. This study is one of them, and will assist in paving the way for future findings. The full spectrum of genetic research – from the identification of mutations in human patients, to the analyses of mechanism and the development of models – represents the direction that must be taken in order to reach the solution underlying the mechanism of LMNA mutations in the pathogenesis of DCM. It is perhaps this path that ultimately holds the greatest promise for advancing the science and treatment of cardiomyopathies.

4.10 Future Directions

It is obvious that more research is needed to elucidate the functional consequences of LMNA mutations in DCM. The results of our RFLP assays have demonstrated that the relative absence of pathology found in the cardiac myocytes of Patient 2 did not correlate with the lack of expression of the R541S LMNA mRNA. One of the next steps is to determine the expression levels of lamin A vs. lamin C in all four chambers of the

heart. This will be accomplished by using Northern blots and quantitative RT-PCR. Although the findings of these experiments will not shed any light directly on a mechanism for DCM, it is a completely novel line of research and may serve as a useful stepping stone for further investigations into the pathogenesis of this disease. For example, although both the D192G and R541S mutations are found within the region of the LMNA gene shared by lamin A and lamin C, it is uncertain whether these mutations will be expressed in only one of these lamins, or both. Consequently, these future experiments may help to determine whether one type of lamin is more prominent than the other in various areas of the heart, which may directly influence the effects of the D192G and R541S mutations, if indeed they are exclusively expressed by either lamin A or lamin C.

Future studies will also delve into the functional consequences of genetic variations in the cardiac tissue of DCM patients and in mutation expression models. Immunohistochemistry will be performed on heart tissue samples in order to determine the location and relative amounts of the mutant and wild-type lamins within the cardiac myocyte. Preliminary results indicate that lamin C with the R541S mutation is correctly targeted to the nucleus, whereas lamin C with the D192G mutation is clearly misdirected to the mitochondria and appears to initiate apoptosis. Lamin degradation has long been recognized as a hallmark of apoptosis, which may be activated in response to a variety of stimuli, including cancer, virus infection, specific drugs, or stress (51;71). In particular, caspase 6 has been identified as the protease responsible for cleaving lamin A at its conserved VEID site, which is located in the non-helical linker region at position 227-230 (51). This step is crucial in order for the chromosomal DNA to undergo complete

condensation during apoptotic execution (63). Studies have shown that caspase cleavage of only a small fraction of A-type lamins is required for its complete disintegration from the nuclear lamina (51). This provides a possible explanation for the discrepancy observed in the ultrastructural phenotype of the cardiac myocytes from these two patients. Time lapse microscopy and fluorescent-tagged proteins will also be used to gain more insight into the trafficking of mutant lamins and their interactions with other proteins inside a cellular model. Finally, animal models, such as mice genetically engineered to possess specific LMNA mutations, will be generated and analyzed to further elucidate the mechanisms underlying the consequences of these mutations in DCM.

5 CONCLUSION

Two novel missense mutations, D192G and R541S, were identified in highly conserved regions of the LMNA gene in two unrelated patients with end-stage dilated cardiomyopathy. Both single nucleotide base substitutions were absent in a population of 100 healthy control individuals. Electron micrographs of the cardiac tissue obtained from the carrier of the D192G mutation (Patient 1) revealed a complete loss of the nuclear membrane and the accumulation of mitochondria in the nuclear matrix. By contrast, examination of the heart tissue sections from the patient with the R541S mutation (Patient 2) revealed only modest and non-specific nuclear membrane alterations, comparable to those found in transplanted DCM patients without LMNA mutations. Quantitative RT-PCR revealed that the expression levels of total LMNA mRNA in Patient 2 were comparable to those found in end-stage DCM patients without LMNA mutations. This suggests that the substitution of arginine by serine in codon 541 did not introduce an element of instability into the mutant LMNA mRNA. In addition, the RFLP assays demonstrated that there was no significant difference between the quantity of R541S vs. wild-type LMNA mRNA expressed in either the left ventricle or the right atria of this patient. Therefore, these experiments conclusively show that the discrepancy observed in the electron micrographs cannot be explained by a lack of expression of the mutant allele. This research provides a basis for further elucidation of the functional consequences of LMNA mutations and their role in the pathogenesis of DCM. Future studies will be directed to assess the impact of these mutations on cellular and animal models.

REFERENCES

1. Seidman, J. G. and Seidman, C. (2001) *Cell* **104**, 557-567
2. Schonberger, J. and Seidman, C. E. (2001) *Am.J.Hum.Genet.* **69**, 249-260
3. Michels, V. V., Moll, P. P., Miller, F. A., Tajik, A. J., Chu, J. S., Driscoll, D. J., Burnett, J. C., Rodeheffer, R. J., Chesebro, J. H., and Tazelaar, H. D. (1992) *N.Engl.J.Med.* **326**, 77-82
4. Taylor, M. R., Fain, P. R., Sinagra, G., Robinson, M. L., Robertson, A. D., Carniel, E., Di Lenarda, A., Bohlmeier, T. J., Ferguson, D. A., Brodsky, G. L., Boucek, M. M., Lascor, J., Moss, A. C., Li, W. L., Stetler, G. L., Muntoni, F., Bristow, M. R., and Mestroni, L. (2003) *J.Am.Coll.Cardiol.* **41**, 771-780
5. Graham, R. M. and Owens, W. A. (1999) *N.Engl.J.Med.* **341**, 1759-1762
6. Pauschinger, M., Knopf, D., Petschauer, S., Doerner, A., Poller, W., Schwimmbeck, P. L., Kuhl, U., and Schultheiss, H. P. (1999) *Circulation* **99**, 2750-2756
7. Tesson, F., Sylvius, N., Pilotto, A., Dubosq-Bidot, L., Peuchmaurd, M., Bouchier, C., Benaiche, A., Mangin, L., Charron, P., Gavazzi, A., Tavazzi, L., Arbustini, E., and Komajda, M. (2000) *Eur.Heart J.* **21**, 1872-1876
8. Kamisago, M., Sharma, S. D., DePalma, S. R., Solomon, S., Sharma, P., McDonough, B., Smoot, L., Mullen, M. P., Woolf, P. K., Wigle, E. D., Seidman, J. G., and Seidman, C. E. (2000) *N.Engl.J.Med.* **343**, 1688-1696
9. Tsubata, S., Bowles, K. R., Vatta, M., Zintz, C., Titus, J., Muhonen, L., Bowles, N. E., and Towbin, J. A. (2000) *J.Clin.Invest* **106**, 655-662
10. Mestroni, L., Rocco, C., Gregori, D., Sinagra, G., Di Lenarda, A., Miocic, S., Vatta, M., Pinamonti, B., Muntoni, F., Caforio, A. L., McKenna, W. J., Falaschi, A., Giacca, M., and Camerini (1999) *J.Am.Coll.Cardiol.* **34**, 181-190
11. Hershberger, R. E., Hanson, E. L., Jakobs, P. M., Keegan, H., Coates, K., Bousman, S., and Litt, M. (2002) *Am.Heart J.* **144**, 1081-1086
12. Feng, J., Yan, J., Buzin, C. H., Towbin, J. A., and Sommer, S. S. (2002) *Mol.Genet.Metab* **77**, 119-126
13. Olson, T. M., Illenberger, S., Kishimoto, N. Y., Huttelmaier, S., Keating, M. T., and Jockusch, B. M. (2002) *Circulation* **105**, 431-437

14. Olson, T. M., Michels, V. V., Thibodeau, S. N., Tai, Y. S., and Keating, M. T. (1998) *Science* **280**, 750-752
15. Bowles, N. E., Bowles, K. R., and Towbin, J. A. (2000) *Herz* **25**, 168-175
16. Karkkainen, S., Peuhkurinen, K., Jaaskelainen, P., Miettinen, R., Karkkainen, P., Kuusisto, J., and Laakso, M. (2002) *Am.Heart J.* **143**, E6
17. Li, D., Tapscoft, T., Gonzalez, O., Burch, P. E., Quinones, M. A., Zoghbi, W. A., Hill, R., Bachinski, L. L., Mann, D. L., and Roberts, R. (1999) *Circulation* **100**, 461-464
18. Takai, E., Akita, H., Shiga, N., Kanazawa, K., Yamada, S., Terashima, M., Matsuda, Y., Iwai, C., Kawai, K., Yokota, Y., and Yokoyama, M. (1999) *Am.J.Med.Genet.* **86**, 325-327
19. Mayosi, B. M., Khogali, S., Zhang, B., and Watkins, H. (1999) *J.Med.Genet.* **36**, 796-797
20. Daehmlow, S., Erdmann, J., Knueppel, T., Gille, C., Froemmel, C., Hummel, M., Hetzer, R., and Regitz-Zagrosek, V. (2002) *Biochem.Biophys.Res.Commun.* **298**, 116-120
21. Hanson, E. L., Jakobs, P. M., Keegan, H., Coates, K., Bousman, S., Diemel, N. H., Litt, M., and Hershberger, R. E. (2002) *J.Card Fail.* **8**, 28-32
22. Li, D., Czernuszewicz, G. Z., Gonzalez, O., Tapscott, T., Karibe, A., Durand, J. B., Brugada, R., Hill, R., Gregoritch, J. M., Anderson, J. L., Quinones, M., Bachinski, L. L., and Roberts, R. (2001) *Circulation* **104**, 2188-2193
23. Hinkle, A., Goranson, A., Butters, C. A., and Tobacman, L. S. (1999) *J.Biol.Chem.* **274**, 7157-7164
24. Olson, T. M., Kishimoto, N. Y., Whitby, F. G., and Michels, V. V. (2001) *J.Mol.Cell Cardiol.* **33**, 723-732
25. Blanchard, E. M., Iizuka, K., Christe, M., Conner, D. A., Geisterfer-Lowrance, A., Schoen, F. J., Maughan, D. W., Seidman, C. E., and Seidman, J. G. (1997) *Circ.Res.* **81**, 1005-1010
26. Gerull, B., Gramlich, M., Atherton, J., McNabb, M., Trombitas, K., Sasse-Klaassen, S., Seidman, J. G., Seidman, C., Granzier, H., Labeit, S., Frenneaux, M., and Thierfelder, L. (2002) *Nat.Genet.* **30**, 201-204
27. Itoh-Satoh, M., Hayashi, T., Nishi, H., Koga, Y., Arimura, T., Koyanagi, T., Takahashi, M., Hohda, S., Ueda, K., Nouchi, T., Hiroe, M., Marumo, F., Imaizumi, T., Yasunami, M., and Kimura, A. (2002) *Biochem.Biophys.Res.Commun.* **291**, 385-393

28. Knoll, R., Hoshijima, M., Hoffman, H. M., Person, V., Lorenzen-Schmidt, I., Bang, M. L., Hayashi, T., Shiga, N., Yasukawa, H., Schaper, W., McKenna, W., Yokoyama, M., Schork, N. J., Omens, J. H., McCulloch, A. D., Kimura, A., Gregorio, C. C., Poller, W., Schaper, J., Schultheiss, H. P., and Chien, K. R. (2002) *Cell* **111**, 943-955
29. Arber, S., Hunter, J. J., Ross, J., Jr., Hongo, M., Sansig, G., Borg, J., Perriard, J. C., Chien, K. R., and Caroni, P. (1997) *Cell* **88**, 393-403
30. Granzier, H. L. and Irving, T. C. (1995) *Biophys.J.* **68**, 1027-1044
31. Milner, D. J., Weitzer, G., Tran, D., Bradley, A., and Capetanaki, Y. (1996) *J.Cell Biol.* **134**, 1255-1270
32. Miyamoto, Y., Akita, H., Shiga, N., Takai, E., Iwai, C., Mizutani, K., Kawai, H., Takarada, A., and Yokoyama, M. (2001) *Eur.Heart J.* **22**, 2284-2289
33. Towbin, J. A., Hejtmancik, J. F., Brink, P., Gelb, B., Zhu, X. M., Chamberlain, J. S., McCabe, E. R., and Swift, M. (1993) *Circulation* **87**, 1854-1865
34. Ferlini, A., Galie, N., Merlini, L., Sewry, C., Branzi, A., and Muntoni, F. (1998) *Am.J.Hum.Genet.* **63**, 436-446
35. Muntoni, F., Di Lenarda, A., Porcu, M., Sinagra, G., Mateddu, A., Marrosu, G., Ferlini, A., Cau, M., Milasin, J., Melis, M. A., Marrosu, M. G., Cianchetti, C., Sanna, A., Falaschi, A., Camerini, F., Giacca, M., and Mestroni, L. (1997) *Heart* **78**, 608-612
36. Ortiz-Lopez, R., Li, H., Su, J., Goytia, V., and Towbin, J. A. (1997) *Circulation* **95**, 2434-2440
37. Sylvius, N., Duboscq-Bidot, L., Bouchier, C., Charron, P., Benaiche, A., Sebillon, P., Komajda, M., and Villard, E. (2003) *Am.J.Med.Genet.* **120A**, 8-12
38. Kawada, T., Nakatsuru, Y., Sakamoto, A., Koizumi, T., Shin, W. S., Okai-Matsuo, Y., Suzuki, J., Uehara, Y., Nakazawa, M., Sato, H., Ishikawa, T., and Toyooka, T. (1999) *FEBS Lett.* **458**, 405-408
39. Xu, W., Baribault, H., and Adamson, E. D. (1998) *Development* **125**, 327-337
40. Maeda, M., Holder, E., Lowes, B., Valent, S., and Bies, R. D. (1997) *Circulation* **95**, 17-20
41. D'Adamo, P., Fassone, L., Gedeon, A., Janssen, E. A., Bione, S., Bolhuis, P. A., Barth, P. G., Wilson, M., Haan, E., Orstavik, K. H., Patton, M. A., Green, A. J., Zammarchi, E., Donati, M. A., and Toniolo, D. (1997) *Am.J.Hum.Genet.* **61**, 862-867

42. Schmitt, J. P., Kamisago, M., Asahi, M., Li, G. H., Ahmad, F., Mende, U., Kranias, E. G., MacLennan, D. H., Seidman, J. G., and Seidman, C. E. (2003) *Science* **299**, 1410-1413
43. Genschel, J. and Schmidt, H. H. (2000) *Hum.Mutat.* **16**, 451-459
44. Machiels, B. M., Zorenc, A. H., Endert, J. M., Kuijpers, H. J., van Eys, G. J., Ramaekers, F. C., and Broers, J. L. (1996) *J.Biol.Chem.* **271**, 9249-9253
45. Mounkes, L. C., Kozlov, S., Hernandez, L., Sullivan, T., and Stewart, C. L. (2003) *Nature* **423**, 298-301
46. Fisher, D. Z., Chaudhary, N., and Blobel, G. (1986) *Proc.Natl.Acad.Sci.U.S.A* **83**, 6450-6454
47. Hutchison, C. J., Alvarez-Reyes, M., and Vaughan, O. A. (2001) *J.Cell Sci.* **114**, 9-19
48. Stuurman, N., Heins, S., and Aebi, U. (1998) *J.Struct.Biol.* **122**, 42-66
49. Wilson, K. L. (2000) *Trends Cell Biol.* **10**, 125-129
50. Holaska, J. M., Wilson, K. L., and Mansharamani, M. (2002) *Curr.Opin.Cell Biol.* **14**, 357-364
51. Broers, J. L., Bronnenberg, N. M., Kuijpers, H. J., Schutte, B., Hutchison, C. J., and Ramaekers, F. C. (2002) *Eur.J.Cell Biol.* **81**, 677-691
52. Raharjo, W. H., Enarson, P., Sullivan, T., Stewart, C. L., and Burke, B. (2001) *J.Cell Sci.* **114**, 4447-4457
53. Bonne, G., Di Barletta, M. R., Varnous, S., Becane, H. M., Hammouda, E. H., Merlini, L., Muntoni, F., Greenberg, C. R., Gary, F., Urtizberea, J. A., Duboc, D., Fardeau, M., Toniolo, D., and Schwartz, K. (1999) *Nat.Genet.* **21**, 285-288
54. Bonne, G., Mercuri, E., Muchir, A., Urtizberea, A., Becane, H. M., Recan, D., Merlini, L., Wehnert, M., Boor, R., Reuner, U., Vorgerd, M., Wicklein, E. M., Eymard, B., Duboc, D., Penisson-Besnier, I., Cuisset, J. M., Ferrer, X., Desguerre, I., Lacombe, D., Bushby, K., Pollitt, C., Toniolo, D., Fardeau, M., Schwartz, K., and Muntoni, F. (2000) *Ann.Neurol.* **48**, 170-180
55. Krimm, I., Ostlund, C., Gilquin, B., Couprie, J., Hossenlopp, P., Mornon, J. P., Bonne, G., Courvalin, J. C., Worman, H. J., and Zinn-Justin, S. (2002) *Structure.(Camb.)* **10**, 811-823
56. Clements, L., Manilal, S., Love, D. R., and Morris, G. E. (2000) *Biochem.Biophys.Res.Commun.* **267**, 709-714

57. Moir, R. D., Spann, T. P., Lopez-Soler, R. I., Yoon, M., Goldman, A. E., Khuon, S., and Goldman, R. D. (2000) *J.Struct.Biol.* **129**, 324-334
58. Moir, R. D., Montag-Lowy, M., and Goldman, R. D. (1994) *J.Cell Biol.* **125**, 1201-1212
59. Pugh, G. E., Coates, P. J., Lane, E. B., Raymond, Y., and Quinlan, R. A. (1997) *J.Cell Sci.* **110 (Pt 19)**, 2483-2493
60. Jagatheesan, G., Thanumalayan, S., Muralikrishna, B., Rangaraj, N., Karande, A. A., and Parnaik, V. K. (1999) *J.Cell Sci.* **112 (Pt 24)**, 4651-4661
61. Goldman, A. E., Moir, R. D., Montag-Lowy, M., Stewart, M., and Goldman, R. D. (1992) *J.Cell Biol.* **119**, 725-735
62. Sullivan, T., Escalante-Alcalde, D., Bhatt, H., Anver, M., Bhat, N., Nagashima, K., Stewart, C. L., and Burke, B. (1999) *J.Cell Biol.* **147**, 913-920
63. Ruchaud, S., Korfali, N., Villa, P., Kottke, T. J., Dingwall, C., Kaufmann, S. H., and Earnshaw, W. C. (2002) *EMBO J.* **21**, 1967-1977
64. Glass, C. A., Glass, J. R., Taniura, H., Hasel, K. W., Blevitt, J. M., and Gerace, L. (1993) *EMBO J.* **12**, 4413-4424
65. Taniura, H., Glass, C., and Gerace, L. (1995) *J.Cell Biol.* **131**, 33-44
66. Rzepecki, R., Bogachev, S. S., Kokoza, E., Stuurman, N., and Fisher, P. A. (1998) *J.Cell Sci.* **111 (Pt 1)**, 121-129
67. Zheng, R., Ghirlando, R., Lee, M. S., Mizuuchi, K., Krause, M., and Craigie, R. (2000) *Proc.Natl.Acad.Sci.U.S.A* **97**, 8997-9002
68. Gotzmann, J. and Foisner, R. (1999) *Crit Rev.Eukaryot.Gene Expr.* **9**, 257-265
69. Maraldi, N. M., Lattanzi, G., Sabatelli, P., Ognibene, A., and Squarzony, S. (2002) *Neuromuscul.Disord.* **12**, 815-823
70. Worman, H. J. and Courvalin, J. C. (2002) *Trends Cell Biol.* **12**, 591-598
71. Burke, B. (2001) *J.Cell Biol.* **153**, F5-F7
72. Heald, R. and McKeon, F. (1990) *Cell* **61**, 579-589
73. Peter, M., Nakagawa, J., Doree, M., Labbe, J. C., and Nigg, E. A. (1990) *Cell* **61**, 591-602
74. Moir, R. D., Spann, T. P., Herrmann, H., and Goldman, R. D. (2000) *J.Cell Biol.* **149**, 1179-1192

75. Spann, T. P., Goldman, A. E., Wang, C., Huang, S., and Goldman, R. D. (2002) *J.Cell Biol.* **156**, 603-608
76. Fatkin, D., MacRae, C., Sasaki, T., Wolff, M. R., Porcu, M., Frenneaux, M., Atherton, J., Vidaillet, H. J., Jr., Spudich, S., De Girolami, U., Seidman, J. G., Seidman, C., Muntoni, F., Muehle, G., Johnson, W., and McDonough, B. (1999) *N.Engl.J.Med.* **341**, 1715-1724
77. Martelli, A. M., Bortul, R., Tabellini, G., Faenza, I., Cappellini, A., Bareggi, R., Manzoli, L., and Cocco, L. (2002) *J.Cell Biochem.* **86**, 320-330
78. Thompson, L. J. and Fields, A. P. (1996) *J.Biol.Chem.* **271**, 15045-15053
79. Shimizu, T., Cao, C. X., Shao, R. G., and Pommier, Y. (1998) *J.Biol.Chem.* **273**, 8669-8674
80. Morris, G. E. (2001) *Trends Mol.Med.* **7**, 572-577
81. Emery, A. E. (2002) *Lancet* **359**, 687-695
82. Raffaele, D. B., Ricci, E., Galluzzi, G., Tonali, P., Mora, M., Morandi, L., Romorini, A., Voit, T., Orstavik, K. H., Merlini, L., Trevisan, C., Biancalana, V., Housmanowa-Petrusewicz, I., Bione, S., Ricotti, R., Schwartz, K., Bonne, G., and Toniolo, D. (2000) *Am.J.Hum.Genet.* **66**, 1407-1412
83. Felice, K. J., Schwartz, R. C., Brown, C. A., Leicher, C. R., and Grunnet, M. L. (2000) *Neurology* **55**, 275-280
84. Markiewicz, E., Venables, R., Mauricio, A. R., Quinlan, R., Dorobek, M., Hausmanowa-Petrusewicz, I., and Hutchison, C. (2002) *J.Struct.Biol.* **140**, 241-253
85. Fidzianska, A., Toniolo, D., and Hausmanowa-Petrusewicz, I. (1998) *J.Neurol.Sci.* **159**, 88-93
86. Muchir, A., Bonne, G., van der Kooij, A. J., van Meegen, M., Baas, F., Bolhuis, P. A., de Visser, M., and Schwartz, K. (2000) *Hum.Mol.Genet.* **9**, 1453-1459
87. Ki, C. S., Hong, J. S., Jeong, G. Y., Ahn, K. J., Choi, K. M., Kim, D. K., and Kim, J. W. (2002) *J.Hum.Genet.* **47**, 225-228
88. Garg, A. (2000) *Am.J.Med.* **108**, 143-152
89. Cao, H. and Hegele, R. A. (2000) *Hum.Mol.Genet.* **9**, 109-112
90. Speckman, R. A., Garg, A., Du, F., Bennett, L., Veile, R., Arioglu, E., Taylor, S. I., Lovett, M., and Bowcock, A. M. (2000) *Am.J.Hum.Genet.* **66**, 1192-1198

91. Shackleton, S., Lloyd, D. J., Jackson, S. N., Evans, R., Niermeijer, M. F., Singh, B. M., Schmidt, H., Brabant, G., Kumar, S., Durrington, P. N., Gregory, S., O'Rahilly, S., and Trembath, R. C. (2000) *Nat. Genet.* **24**, 153-156
92. Araujo-Vilar, D., Loidi, L., Dominguez, F., and Cabezas-Cerrato, J. (2003) *Horm. Metab Res.* **35**, 29-35
93. Peters, J. M., Barnes, R., Bennett, L., Gitomer, W. M., Bowcock, A. M., and Garg, A. (1998) *Nat. Genet.* **18**, 292-295
94. Hegele, R. A., Anderson, C. M., Wang, J., Jones, D. C., and Cao, H. (2000) *Genome Res.* **10**, 652-658
95. Hegele, R. A., Cao, H., Huff, M. W., and Anderson, C. M. (2000) *J. Clin. Endocrinol. Metab* **85**, 3089-3093
96. Holt, I., Clements, L., Manilal, S., Brown, S. C., and Morris, G. E. (2001) *Eur. J. Hum. Genet.* **9**, 204-208
97. Vigouroux, C., Magre, J., Vantyghem, M. C., Bourut, C., Lascols, O., Shackleton, S., Lloyd, D. J., Guerci, B., Padova, G., Valensi, P., Grimaldi, A., Piquemal, R., Touraine, P., Trembath, R. C., and Capeau, J. (2000) *Diabetes* **49**, 1958-1962
98. Hegele, R. A., Cao, H., Anderson, C. M., and Hramiak, I. M. (2000) *J. Clin. Endocrinol. Metab* **85**, 3431-3435
99. Chaouch, M., Allal, Y., Sandre-Giovannoli, A., Vallat, J. M., Amer-el-Khedoud, A., Kassouri, N., Chaouch, A., Sindou, P., Hammadouche, T., Tazir, M., Levy, N., and Grid, D. (2003) *Neuromuscul. Disord.* **13**, 60-67
100. Sandre-Giovannoli, A., Chaouch, M., Kozlov, S., Vallat, J. M., Tazir, M., Kassouri, N., Szepetowski, P., Hammadouche, T., Vandenberghe, A., Stewart, C. L., Grid, D., and Levy, N. (2002) *Am. J. Hum. Genet.* **70**, 726-736
101. Bouhouche, A., Benomar, A., Birouk, N., Mularoni, A., Meggouh, F., Tassin, J., Grid, D., Vandenberghe, A., Yahyaoui, M., Chkili, T., Brice, A., and LeGuern, E. (1999) *Am. J. Hum. Genet.* **65**, 722-727
102. Novelli, G., Muchir, A., Sangiuolo, F., Helbling-Leclerc, A., D'Apice, M. R., Massart, C., Capon, F., Sbraccia, P., Federici, M., Lauro, R., Tudisco, C., Pallotta, R., Scarano, G., Dallapiccola, B., Merlini, L., and Bonne, G. (2002) *Am. J. Hum. Genet.* **71**, 426-431
103. Eriksson, M., Brown, W. T., Gordon, L. B., Glynn, M. W., Singer, J., Scott, L., Erdos, M. R., Robbins, C. M., Moses, T. Y., Berglund, P., Dutra, A., Pak, E., Durkin, S., Csoka, A. B., Boehnke, M., Glover, T. W., and Collins, F. S. (2003) *Nature* **423**, 293-298

104. Cao, H. and Hegele, R. A. (2003) *J.Hum.Genet.* **48**, 271-274
105. Sandre-Giovannoli, A., Bernard, R., Cau, P., Navarro, C., Amiel, J., Boccaccio, I., Lyonnet, S., Stewart, C. L., Munnich, A., Le Merrer, M., and Levy, N. (2003) *Science* **300**, 2055
106. Mestroni, L., Maisch, B., McKenna, W. J., Schwartz, K., Charron, P., Rocco, C., Tesson, F., Richter, A., Wilke, A., and Komajda, M. (1999) *Eur.Heart J.* **20**, 93-102
107. Henry, W. L., DeMaria, A., Gramiak, R., King, D. L., Kisslo, J. A., Popp, R. L., Sahn, D. J., Schiller, N. B., Tajik, A., Teichholz, L. E., and Weyman, A. E. (1980) *Circulation* **62**, 212-217
108. Manolio, T. A., Baughman, K. L., Rodeheffer, R., Pearson, T. A., Bristow, J. D., Michels, V. V., Abelmann, W. H., and Harlan, W. R. (1992) *Am.J.Cardiol.* **69**, 1458-1466
109. Maisch, B. (1996) *Herz* **21**, 207-212
110. Miller, S. A., Dykes, D. D., and Polesky, H. F. (1988) *Nucleic Acids Res.* **16**, 1215
111. Brodsky, G. L., Muntoni, F., Miocic, S., Sinagra, G., Sewry, C., and Mestroni, L. (2000) *Circulation* **101**, 473-476
112. Jakobs, P. M., Hanson, E. L., Crispell, K. A., Toy, W., Keegan, H., Schilling, K., Icenogle, T. B., Litt, M., and Hershberger, R. E. (2001) *J.Card Fail.* **7**, 249-256
113. Arbustini, E., Pilotto, A., Repetto, A., Grasso, M., Negri, A., Diegoli, M., Campana, C., Scelsi, L., Baldini, E., Gavazzi, A., and Tavazzi, L. (2002) *J.Am.Coll.Cardiol.* **39**, 981-990
114. Charniot, J. C., Pascal, C., Bouchier, C., Sebillon, P., Salama, J., Duboscq-Bidot, L., Peuchmaurd, M., Desnos, M., Artigou, J. Y., and Komajda, M. (2003) *Hum.Mutat.* **21**, 473-481
115. Lin, F. and Worman, H. J. (1993) *J.Biol.Chem.* **268**, 16321-16326
116. Beck, L. A., Hosick, T. J., and Sinensky, M. (1990) *J.Cell Biol.* **110**, 1489-1499
117. Lutz, R. J., Trujillo, M. A., Denham, K. S., Wenger, L., and Sinensky, M. (1992) *Proc.Natl.Acad.Sci.U.S.A* **89**, 3000-3004
118. Herrmann, H. and Aepli, U. (1998) *Curr.Opin.Struct.Biol.* **8**, 177-185
119. Mounkes, L. C., Burke, B., and Stewart, C. L. (2001) *Trends Cardiovasc.Med.* **11**, 280-285

120. Lin, F., Blake, D. L., Callebaut, I., Skerjanc, I. S., Holmer, L., McBurney, M. W., Paulin-Levasseur, M., and Worman, H. J. (2000) *J.Biol.Chem.* **275**, 4840-4847
121. Sewry, C. A., Brown, S. C., Mercuri, E., Bonne, G., Feng, L., Camici, G., Morris, G. E., and Muntoni, F. (2001) *Neuropathol.Appl.Neurobiol.* **27**, 281-290
122. Vigouroux, C., Auclair, M., Dubosclard, E., Pouchelet, M., Capeau, J., Courvalin, J. C., and Buendia, B. (2001) *J.Cell Sci.* **114**, 4459-4468
123. Lenz-Bohme, B., Wismar, J., Fuchs, S., Reifegerste, R., Buchner, E., Betz, H., and Schmitt, B. (1997) *J.Cell Biol.* **137**, 1001-1016
124. Becane, H. M., Bonne, G., Varnous, S., Muchir, A., Ortega, V., Hammouda, E. H., Urtizbera, J. A., Lavergne, T., Fardeau, M., Eymard, B., Weber, S., Schwartz, K., and Duboc, D. (2000) *Pacing Clin.Electrophysiol.* **23**, 1661-1666
125. Ostlund, C., Bonne, G., Schwartz, K., and Worman, H. J. (2001) *J.Cell Sci.* **114**, 4435-4445
126. Hegele, R. A. (2000) *Nat.Med.* **6**, 136-137
127. Furukawa, K. (1999) *J.Cell Sci.* **112 (Pt 15)**, 2485-2492
128. Ye, Q., Callebaut, I., Pezhman, A., Courvalin, J. C., and Worman, H. J. (1997) *J.Biol.Chem.* **272**, 14983-14989
129. Stewart, C. and Burke, B. (1987) *Cell* **51**, 383-392
130. Rober, R. A., Weber, K., and Osborn, M. (1989) *Development* **105**, 365-378
131. van der Kooi, A. J., Bonne, G., Eymard, B., Duboc, D., Talim, B., Van, d., V, Reiss, P., Richard, P., Demay, L., Merlini, L., Schwartz, K., Busch, H. F., and de Visser, M. (2002) *Neurology* **59**, 620-623
132. Garg, A., Speckman, R. A., and Bowcock, A. M. (2002) *Am.J.Med.* **112**, 549-555
133. Battistella, P. A., Moreolo, G. S., Benetti, E., Da Dalt, L., and Pellegrino, P. A. (1988) *Brain Dev.* **10**, 262-263
134. Ichihara, S., Yamada, Y., and Yokota, M. (1998) *Circulation* **98**, 1881-1885
135. Hiroi, S., Harada, H., Nishi, H., Satoh, M., Nagai, R., and Kimura, A. (1999) *Biochem.Biophys.Res.Commun.* **261**, 332-339
136. Arimura, T., Nakamura, T., Hiroi, S., Satoh, M., Takahashi, M., Ohbuchi, N., Ueda, K., Nouchi, T., Yamaguchi, N., Akai, J., Matsumori, A., Sasayama, S., and Kimura, A. (2000) *Hum.Genet.* **107**, 440-451

137. Tiago, A. D., Badenhorst, D., Skudicky, D., Woodiwiss, A. J., Candy, G. P., Brooksbank, R., Sliwa, K., Sareli, P., and Norton, G. R. (2002) *Cardiovasc.Res.* **54**, 584-589
138. MacRae, C. A. (2000) *Eur.Heart J.* **21**, 1817-1819
139. Arbustini, E., Morbini, P., Pilotto, A., Gavazzi, A., and Tavazzi, L. (2000) *Eur.Heart J.* **21**, 1825-1832
140. Schmidt, H. H. and Lochs, H. (2001) *Circulation* **103**, E20
141. Kumaran, R.I., Muralikrishna, B., Parnaik, V.K. (2002) *J. Cell. Biol.* **159**, 783-93

6 CONTRIBUTIONS OF COLLABORATORS

The DCM patients in this study were recruited by our clinical research coordinators, Angelina Jipson and Michaela Garkisch, in collaboration with members of the University of Ottawa Heart Institute cardiology division. DNA and tissue samples were also obtained from the National Institute of Cardiology in Warsaw, Poland with the cooperation of Drs. Bilinska and Ruzyllo.

Screening for novel LMNA mutations was performed with the assistance of Pierrette Bolongo. Myocardial ultrastructural changes were assessed in collaboration with Dr. Veinot, from the University of Ottawa, and Dr. Fidzianska, from the Polish Academy of Science in Warsaw, Poland. In addition, the vectors used to construct the standard curves for the quantitative RT-PCR experiments were kindly provided by André Gauthier and Pierrette Bolongo.

APPENDIX 1

Familial DCM Genes

Locus	Trait	Additional Phenotype	Disease Gene	Protein Function
1q32	AD	none	cardiac troponin T	-one component of a ternary complex of proteins (troponins T, C, and I) -transmits calcium signals that regulate actin-myosin interactions and ATPase activity
2q31	AD	none	titin	-extend from sarcomeric Z-discs to M-lines -provide an extensible scaffold for contractile machinery, and are crucial for myofibrillar elasticity and integrity
5q33-34	AD	none	delta-sarcoglycan	-component of the dystrophin-associated sarcoglycan complex that forms a structural link between the F-actin cytoskeleton and the extracellular matrix
6q12-16	AD	none	?	
6q22.1	AD	none	phospholamban	-transmembrane phosphoprotein that inhibits the cardiac sarcoplasmic reticular calcium-adenosin triphosphatase (SERCA2a) pump in its unphosphorylated state
9q13-22	AD	none	?	
10q22.1-q23	AD	none	metavinculin	-protein component of intercalated discs, that is expressed exclusively in cardiac and smooth muscle -anchors F-actin to the membrane and transmits contractile force between cardiac myocytes
11p11.2	AD	none	cardiac myosin-binding protein C (MYBPC)	-arrayed transversely in the A-bands of the sarcomere -binds myosin heavy chain in thick filaments and interacts with titin in elastic filaments -phosphorylation of this protein appears to modulate contraction
11p15.1	AD	none	cystein-and glycine-rich protein 3 (MLP)	-intrinsic element of the Z disc -stabilizes titin-cap at the most proximal end of the titin complex

14q11	AD	none	cardiac beta myosin heavy chain	-force generator in muscle contraction
15q14	AD	none	cardiac actin	-major constituent of the contractile apparatus -plays key role in transmitting force between adjacent sarcomeres and neighboring myocytes to effect coordinated contraction of the heart
15q22.1	AD	none	alpha-tropomyosin	-one of the proteins comprising the thin filaments of the sarcomere -undergoes a conformational change upon the binding of calcium to the troponin complex -leads to the disinhibition of interaction between actin and myosin, which generates contractile force
17q12	AD	none	titin-cap	-sarcomeric protein found in the Z disc of adult skeletal muscle and cultured myocytes -substrate of titin
10q21-23	AD	mitral valve prolapse	?	
1p1-q21	AD	conduction disease	lamin A/C	-maintains integrity of the nuclear architecture -provides anchorage sites for chromatin -DNA replication -RNA pol II transcription -signal transduction
2q14-q22	AD	conduction disease	?	
3p22-25	AD	conduction disease	?	
6q23	AD	conduction disease and skeletal myopathy	?	
2q35	AD	skeletal myopathy	desmin	-in mature striated muscle, desmin intermediate filaments surround the Z-discs, link them together, and integrate the contractile apparatus with the sarcolemma and the nucleus
6q23-24	AD	sensorineur	?	

		al hearing loss		
2q32.1-32.3	AD	ARVD	?	
3p23	AD	ARVD	?	
10p12-14	AD	ARVD	?	
14q12-22	AD	ARVD	?	
14q23-24	AD	ARVD	?	
Xp21	X	skeletal myopathy	dystrophin	-large cytoskeletal protein that plays a critical role in membrane stability, force transduction, and organization of the membrane in both skeletal and cardiac myocytes
Xq28	X	short stature and neutropenia	tafazzin	-unknown function

APPENDIX II

Summary of Primers, Annealing Temperatures, and Lengths of PCR Amplicons for LMNA Exons 1-12

Exon	Primer Sequences (5'→3')		Product Length (bp)	PCR Annealing Temperature
	Forward	Reverse		
1A	TCTGTCCTTCGACCCGAG	GTAGACCGCCAAGCGATC	209	50
1B	GGAGGACCTGCAGGAGCT	GCCCTCTCACTCCCTTCC	352	50
2	CAGACTCCTTCTCTAAATCTAC	CCTAGGTAGAAGAGTGAGTGTAC	268	58
3	CCTTCAAGTTCTTGTGTCTGTGAC	CCTAGGTAGAAGAGTGAGTGTAC	250	61
4	GGCCTCCAGGAACCTAATTCTG	CTCCCTGCCACCATCTGC	334	63
5	TCCACCCCTCCAGTCAC	GAACCTCCACCACCACC	428	63
6	ATCCTGGAGAGAGTAGCCAG	TCTAGTCAAGGCCAGTTGCC	293	51
7	CCCCACTTGGTCTCCCTCTCC	CCCTGATGCAGCTGTATCCCC	311	50
8	GAGGCCTCAATTGCAGGCAGGC	GAAAAGGACACTTACCCCAGC	286	62 and 63.1
9	GGAGCGCTGGGGTAAGTGTC	CTCGTCCAGCAAGCAGCCAG	192	48
10	GTAAGCAGCAGGCCGGACAAAG	GATGCCATGGAATATTCTGTG	458	58
11A	GGTCAGTCCCAGACTCGC	ACCAGATTGTCCCCGAAG	276	52
11B	GTCACTCGCAGCTACCGC	CCACCTCGTCTACCCCT	178	52
12	CTTGTCTGAGCCCCAGACTGGAG	AGGGAAAAGGAAGGGAGGAGAAAT	483	65

APPENDIX III

DHPLC Column Temperatures for Each LMNA PCR Amplicon

Exon	DHPLC Column Temperature (°C)
1	66
1A	65
2	63
3	62
4	62
5	61
6	63
7	64
8	62
9	62.3
10	60
11A	65
11B	62.6
12	62

STEPHANIE POON

EDUCATION

- 2002-present **Queen's University:** School of Medicine
 2001-present **University of Ottawa:** Department of Biochemistry, Microbiology and Immunology
 1997-2001 **University of Toronto:** Department of Immunology
 1990-1997 **St. Matthew High School**
 1986-1997 **Conservatoire de Musique du Québec**

DIPLOMAS, DEGREES AND CERTIFICATIONS

- 2001 Hon. B.Sc. with High Distinction
 1997 Ontario Secondary School Diploma (honours)
 1996 Canadian TaeKwon-Do Federation International certification: Class B referee
 1996 Diplôme d'Études Intermédiaires in piano
 1994 Certification: TaeKwon-Do instructor

ACHIEVEMENTS / AWARDS

- 1998-2001 Dean's List Scholar
 1998-2000 Regents In-Course Scholarship
 1998 Canadian TaeKwon-Do Championship: silver medal
 1997 University of Toronto Scholars Entrance Scholarship
 1997 University of Toronto Scholar
 1997 Governor General's Academic Medal
 1997 Ontario Scholar
 1996 Canadian TaeKwon-Do Championship: 2 gold medals, national junior champion
 1996 Canadian Music Competitions, National Final: 2nd place in piano
 1996 guest performer on CBC Radio Young Artists Program
 1995 North American TaeKwon-Do Championships: 4 gold medals
 1995, 1992 Concours CIMF Rock Détente: 1st place
 1993 guest soloist with the Hull Chamber Music Orchestra

WORK EXPERIENCE

- 2000-2001 **Student Researcher**
 Princess Margaret Hospital: Department of Medical Biophysics
- cultured MCF7 and MDA231 human breast cancer cell lines
 - quantified EGFR expressed by MDA231 through fluorimetry and Scatchard analysis
- 2000
 summer **Student Researcher**
 Hospital for Sick Children: Department of Infection, Immunity, Injury and Repair
- generated dendritic cell cultures from bone marrow precursors
 - determined the optimal growth conditions for dendritic cells in a bone marrow culture
 - performed proliferation and cytotoxicity assays to compare the function of cultured dendritic cells at various stages of differentiation
 - conducted experiments which demonstrated that dendritic cells could be transfected
 - used flow cytometry to analyze the phenotype of cultured dendritic cells over varying time periods to characterize the process of differentiation
- 1998
 summer **Greeter**
 Children's Hospital of Eastern Ontario: Department of Security
- answered any questions that incoming patients and their families had about the hospital and directed them to their desired locations
 - wrote reports that summarized the incidents encountered each day
 - trained prospective greeters on how to handle various problems
 - ensured that parking regulations and various other hospital policies were observed by visitors, patients, and their families
- 1997-2001
 summer **Volunteer**
 Children's Hospital of Eastern Ontario
 The Rehabilitation Centre

EXTRA-CURRICULAR ACTIVITIES

- 1982-present • piano
- 1990-2000 • Taekwon-Do, second-degree black belt holder
- 1998-1999 • treasurer of residence council
- 1998-1999 • yoga

REFERENCES

Available upon request